Clim Dyn (2009) 32:143–165
DOI 10.1007/s00382-008-0480-9

Orbital forcing and role of the latitudinal insolation/temperature gradient

Basil A. S. Davis · Simon Brewer

Received: 9 January 2007 / Accepted: 7 October 2008 / Published online: 26 October 2008

Abstract Orbital forcing of the climate system is clearly shown in the Earths record of glacial–interglacial cycles, but the mechanism underlying this forcing is poorly understood. Traditional Milankovitch theory suggests that these cycles are driven by changes in high latitude summer insolation, yet this forcing is dominated by precession, and cannot account for the importance of obliquity in the Ice Age record. Here, we investigate an alternative forcing based on the latitudinal insolation gradient (LIG), which is dominated by both obliquity (in summer) and precession (in winter). The insolation gradient acts on the climate system through differential solar heating, which creates the Earths latitudinal temperature gradient (LTG) that drives the atmospheric and ocean circulation. A new pollen-based reconstruction of the LTG during the Holocene is used to demonstrate that the LTG may be much more sensitive to changes in the LIG than previously thought. From this, it is shown how LIG forcing of the LTG may help explain the propagation of orbital signatures throughout the climate system, including the Monsoon, Arctic Oscillation and ocean circulation. These relationships are validated over the last (Eemian) Interglacial, which occurred under a different orbital configuration to the Holocene. We conclude that LIG forcing of the LTG explains many criticisms of classic Milankovitch theory, while being poorly represented in climate models.

Keywords Orbital forcing · Insolation gradient · Temperature gradient · Milankovitch · Interglacial

B. A. S. Davis
School of Geography, Politics and Sociology,
University of Newcastle, Newcastle upon Tyne NE1 7RU, UK

Present Address:
B. A. S. Davis (✉)
ARVE Group, ISTE, EPFL, 1015 Lausanne, Switzerland
e-mail: basil.davis@epfl.ch

S. Brewer
CEREGE, Europôle de l'Arbois, B.P. 80,
13545 Aix-en-Provence Cedex 04, France

1 Introduction

Regular periodicities in the Earth's orbit and tilt influence the amount and distribution of the sun's energy falling on the Earth. The importance of this orbital forcing on the Earth's climate is clearly illustrated by the close relationship between these periodicities and the Earth's glacial–interglacial cycles (Hays et al. 1976). Spectral analysis of the marine ice volume record (Imbrie et al. 1984) reveals glacial–interglacial cycles vary according to three main periodicities, corresponding to the orbital perturbations associated with eccentricity (100 ka), obliquity (41 ka) and two closely associated precession cycles at 23 and 19 ka (21 ka) (Fig. 1a). Independent validation of this astronomical time-scale has come from radiometric dating of coral reefs and magnetic reversals, providing convincing proof that the Earth's climate and orbit are intimately linked. Yet despite this distinctive signature on the climate record, the identification of the mechanism by which orbital forcing influences the climate system remains unclear.

It has been widely demonstrated (e.g. Imbrie et al. 1992) that the climate system responds linearly (with appropriate lags) to the 41 ka obliquity and 21 ka precession signals. The non-linearity and variable timing apparent in the dominant 100 ka periodicity has led to the conclusion that it arises through a non-linear internally driven response of

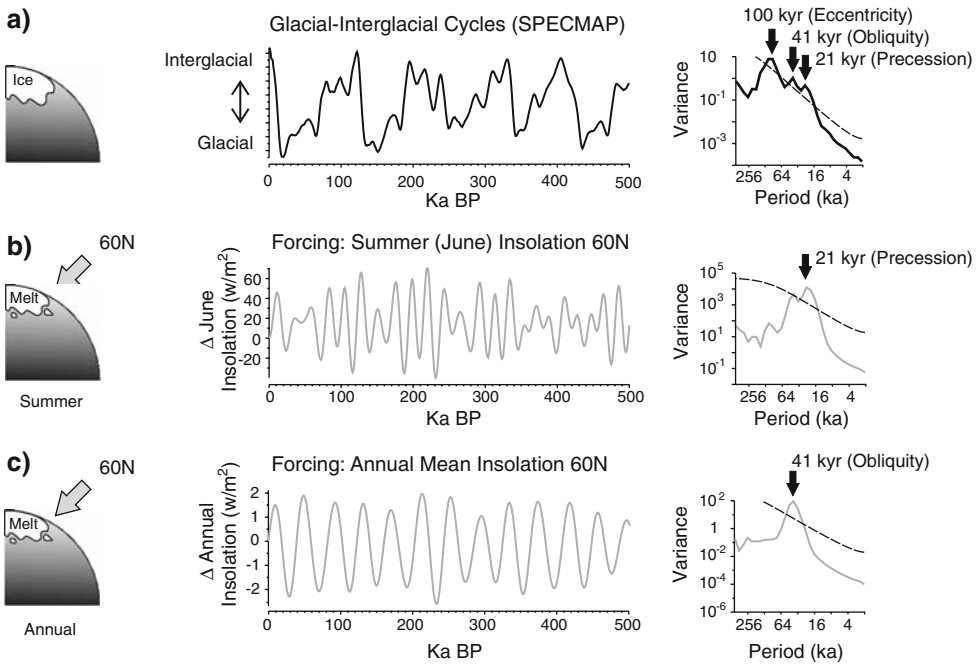

Fig. 1 A comparison of the SPECMAP glacial-interglacial record (Imbrie et al. 1984) with two alternative orbital insolation forcings. Spectral analysis is shown on the right (Torrence and Compo 1998). **a** The SPECMAP glacial–interglacial record shows *peaks* in three main orbital frequencies associated with Eccentricity, Obliquity and Precession, although the 100 ka cycle is considered to result from internal non-linear feedbacks and not Eccentricity (see text). **b** High latitude summer insolation forcing is the most widely accepted orbital forcing (Milankovitch 1930), but this forcing is almost entirely dominated by precession. **c** Annual insolation contains a strong obliquity signal, but the changes are very small

the climate system to the other cycles (Imbrie et al. 1993; Ruddiman 2003). It is not generally considered to represent a direct response to the weak changes in insolation associated with the 100 ka eccentricity cycle. A simple model incorporating the idea of a non-linear internally driven response has successfully reproduced the pattern of 100 ka cycles over the last 0.8 million years (Paillard 1998, 2001; Parrenin and Paillard 2003). Suggested causes of the internal non-linear 100 ka amplifier have included the thermohaline circulation (Imbrie et al. 1993), CO_2 (Shackleton 2000), and ice sheet dynamics (Parrenin and Paillard 2003). External orbital forcing of the climate system has therefore largely been concentrated on understanding the role of the 41 ka obliquity and 21 ka precession cycles.

Without doubt, the most widely accepted explanation of the role of orbital forcing remains Milankovitch Ice Age theory (Milankovitch 1930). This theory suggests glacial–interglacial cycles are driven by the amount of summer insolation falling across high latitude regions where ice sheets develop, a forcing dominated by the 19–23 ka precession cycle (Fig. 1b). But this theory cannot explain: (1) evidence that the onset of the last interglacial occurred before high latitude summer insolation reached significant levels (the 'Stage 5 problem') (Gallup et al. 2002), (2) the presence of an interglacial when high latitude summer insolation failed to reach significant levels at all (the 'Stage 11 problem') (Howard 1997), (3) the synchronisation of interglacials between Hemispheres with opposing insolation receipts (Schrag 2000), and, (4) the lack of precession periodicities in the glacial–interglacial record of the late Pliocene to early Pleistocene ca.3.0–0.8 Ma BP (Raymo and Nisancioglu 2003) and even earlier glacial periods over the last 65 Million years (Zachos et al. 2001). These discrepancies have led to greater interest in the 41 ka obliquity cycle. The importance of obliquity is suggested by the fact it (1) led precession into the last interglacial, (2) was still strong during the Stage 11 interglacial, (3) results in synchronous insolation changes between hemispheres, and (4) dominated the glacial-interglacial record of the early Ice Age Earth.

Two main theories have been forwarded to explain the role of obliquity. The first is through its control of mean annual insolation, and the second through its control of the Earth's latitudinal insolation gradient (LIG). Obliquity controls annual mean insolation at all latitudes (Loutre et al. 2004) although the variance over the obliquity cycle is very small (<3 W/m^2 at 60°N) (Fig. 1c). Nevertheless, annual mean insolation has been forwarded as an explanation for contrary trends in SST observed during the last interglacial north and south of 43°N in the North Atlantic (Cortijo et al. 1999; Loutre et al. 2004). The contrary trends in annual insolation between high and low latitudes is also reflected in a strong obliquity signal in the annual LIG, which along with the SST gradient, has been suggested as the origin of obliquity periodicities evident in the deuterium excess record from both the Vostok ice core in Antarctica (Vimeux et al. 1999), and the GRIP core in Greenland (Masson-Delmotte et al. 2005). Alternatively, Raymo and Nisancioglu (2003) have proposed that obliquity is important because of its influence on the summer LIG (Fig. 2a). The evidence proposed in support of annual

LIG forcing may also be interpreted in support of summer LIG forcing. The SST evidence forwarded by Cortijo et al. (1999) refers mainly to reconstructed August SST's, while the Vostok deuterium excess record is also likely to reflect summer conditions because this is the main period of snowfall in central Antarctica (Reijmer et al. 2002). Snowfall over the smaller Greenland ice sheet is also thought to be primarily in summer during glacial periods, but with a greater contribution in winter during interglacials, when coincidentally the obliquity signal breaks down (Masson-Delmotte et al. 2005). Contrary trends in alkenone derived SST's between high and low latitudes have also been identified during the Holocene by Rimbu et al. (2003), similar to those identified for the Eemian by Cortijo et al. (1999). In this case though, these trends have been explained by changes in tropical winter insolation (Rimbu et al. 2004), which is dominated by precession. In fact, because high latitudes in winter fall under the long polar night, the winter LIG is also dominated by these same changes in low latitude insolation (Fig. 2b). This means that the seasonal LIG is influenced by obliquity in summer and precession in winter, providing both of the main orbital signals found in the glacial–interglacial record.

However, if the LIG was to be influential in driving glacial–interglacial cycles, how could this occur? It has been proposed that the LIG could influence climate through control of the poleward moisture flux, which would influence ice sheet development (Young and Bradley 1984). This idea appears to be supported by the polar deuterium excess records (Vimeux et al. 1999, Masson-Delmotte et al. 2005). A second factor is the role of the LIG on the earth's latitudinal temperature gradient (LTG), and the poleward flux of latent and sensible heat, as proposed by Raymo and Nisancioglu (2003). The LTG arises from differential solar heating between the equator and the poles along the LIG. Incoming radiation exceeds outgoing radiation at low latitudes, while outgoing radiation exceeds incoming radiation at high latitudes. The climate system moves to correct this energy imbalance by transporting energy from warm low latitudes to cold high latitudes via the atmospheric circulation and (wind driven) ocean currents. The LIG therefore provides first order forcing of the LTG, which drives the poleward energy flux via the atmospheric and ocean circulation. The importance of this mechanism on high latitude climate is illustrated by the fact direct solar heating only makes up around half the annual energy budget of high latitudes, with the remainder coming from energy imports from low latitudes (Peixoto and Oort 1992). The LTG also has a wider impact on the climate system by influencing the intensity and position of mid-latitude storms, the tropical Hadley Cell, sub-tropical high and sub-polar low pressure centres (Rind 1998; Jain et al. 1999), as well as polar amplification of changes in mean temperature (forced by Greenhouse gases).

The LTG has been compared in importance to the mean global temperature as a diagnostic of the climate system (Lindzen 1994), yet this feature of the Earths climate remains poorly studied, especially on longer orbital timescales. A major factor has been the continued paucity of temperature records from low latitudes relative to high latitudes, a problem that has inevitably given us a polar centric view of past global climate change. A further difficulty is the limited number of winter temperature records, a factor that has restricted our view of the climate system

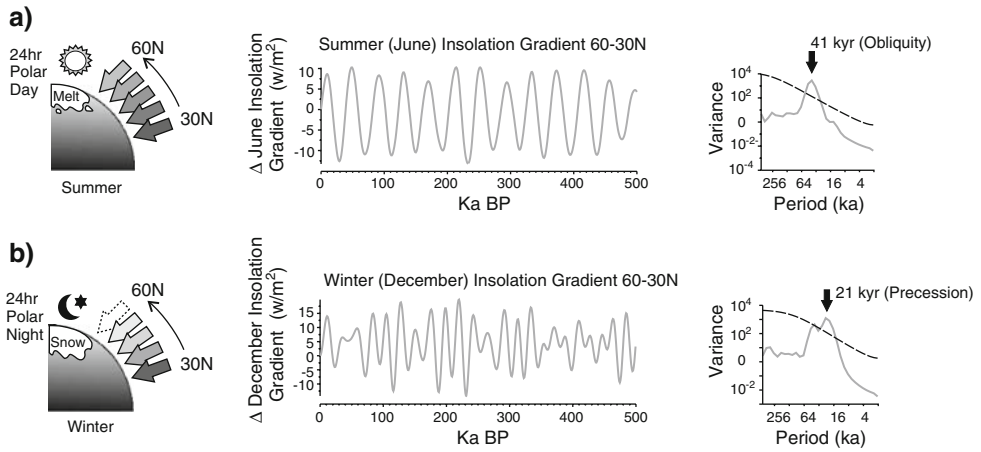

Fig. 2 The latitudinal insolation gradient (LIG) contains both obliquity and precession frequencies found in the glacial-interglacial record as a result of seasonal differences in orbital forcing. Spectral analysis is shown on the *right* (Torrence and Compo 1998) **a** In summer the LIG is dominated by the 41 ka obliquity signal because insolation is strong even at high latitudes where 24 h polar day is experienced. **b** In winter the LIG is dominated by the 21 ka precession signal because the high latitude 24 h polar night means the gradient is controlled by variations in low latitude insolation, which is dominated by precession

over the full seasonal cycle. Here, we have tackled these problems to investigate LIG forcing of the LTG by using a pollen-based gridded climate record to estimate the Northern Hemisphere LTG during the Holocene between the Scandinavian Arctic and African sub-tropics. This record also provides a continuous view of the LTG in both winter and summer, allowing us to compare changes in the LTG against the seasonally distinct orbital signature of the LIG, which varies with obliquity in summer and precession in winter. We validate the LTG reconstruction based on comparison with proxy records of the main climate modes that would be expected to be influenced by the LTG during the Holocene, such as the summer Monsoon and winter Arctic Oscillation (AO). From this analysis, we are able to estimate the pre-Holocene LTG which we further validate against observational data for the same climate mode proxies during the last Eemian interglacial, which occurred under a contrasting orbital configuration.

2 The Holocene interglacial

2.1 The mid-Holocene LTG and LIG

Long standing support for Milankovitch ice age theory has come from the observation that pre-industrial Holocene temperatures peaked during the mid-Holocene 'thermal optimum', when Northern Hemisphere summer insolation was higher than present, and LGM ice sheets had already melted back to modern levels (COHMAP 1988). Evidence of high latitude warming at this time is extensive (eg. Kerwin et al. 1999), consistent with Milankovitch's idea that deglaciation was driven by high latitude warming due to increased summer insolation arising from exaggeration of the seasonal insolation cycle by orbital changes in precession. Yet despite increased summer insolation across all latitudes of the Northern Hemisphere during the mid-Holocene, there is little or no evidence that low latitudes underwent warming in the same way as high latitudes. Rather, evidence from both marine sst's (Rimbu et al. 2003; Rimbu et al. 2004) and terrestrial proxies (Masson et al. 1999; Sawada et al. 2004; Peyron et al. 2000; Beyerle et al. 2003) indicates widespread low latitude cooling that is contrary to the increase in summer insolation.

A compilation of mid-Holocene temperature reconstructions by latitude at 6 ka BP illustrates the contrast between high latitudes where temperatures were warmer than present and low latitudes where temperatures were largely cooler than present (Fig. 3a). These records generally reflect summer temperature conditions; although, we also include a geothermal record from Greenland and alkenone SST records for comparison, which can be expected to record annual temperatures. Where proxies reconstruct warmest/coldest month, summer is assumed to be represented by the warmest month except for areas of the tropics where summer generally coincides with the cooler wet season. This is the case for Tropical East Africa, and we have therefore used the coldest month anomalies in the case of the reconstruction by Peyron et al. (2000). In fact seasonal insolation and seasonal temperature changes are limited at low latitudes, and there are few differences between coldest and warmest month anomalies in the Peyron et al. (2000) reconstruction (see also Fig. 9).

An important additional factor in considering terrestrial temperature anomalies at this time is the role of changing lapse rates. A weakened vertical temperature gradient would be expected to accompany a weakened LTG (Rind 1998). Weaker mid-Holocene lapse rates have been identified by Peyron et al. (2000) in tropical East Africa, and by Huntley and Prentice (1988) in the European Alps. We illustrate these changes in Fig. 3b, with pollen derived temperature anomalies for sites arranged by altitude from tropical East Africa (Peyron et al. 2000), and Southern Europe (Davis et al. 2003). Correlations between temperature change and altitude for both regions are significant within the errors shown (Southern Europe $P = 0.0000$, East Africa $P = 0.0005$). Since the major part of the land surface is at lower altitudes (87% lies below 2,000 m), these lapse rate changes show how reconstructions based on high altitude sites could lead to bias, particularly when comparing with climate models which use a low resolution mean topography at the grid box scale.

It is for this reason that sites from tropical East Africa above 2,000 m from the Peyron et al. (2000) reconstruction have been omitted in Fig. 4a. The data for Europe from Davis et al. (2003) in Figs. 3a and 4a (and subsequent figures) is based on a 3-dimensional gridding procedure which explicitly takes into account any lapse rate changes (Davis et al. 2003). With the omission of the low latitude, high altitude data in Fig. 4a, it becomes clear that observational evidence of low latitude surface cooling at the same time as high latitude warming indicates that weakening of the LTG during the mid-Holocene was not simply based on high latitude warming. This evidence of low latitude summer cooling does not equate easily with increased summer insolation across all latitudes of the Northern Hemisphere during the mid-Holocene (Fig. 4a), which would be expected to cause a widespread increase in summer temperatures even at low latitudes. Rather, low latitude cooling appears to equate better with a weakening of the summer LIG during the mid-Holocene, and consequent weakening of the LTG. The weakened gradient reflects a proportionally greater increase in insolation at high latitudes compared to low latitudes during the mid-Holocene. This is shown in Fig. 4a where low latitudes received less than the mean June increase in insolation of

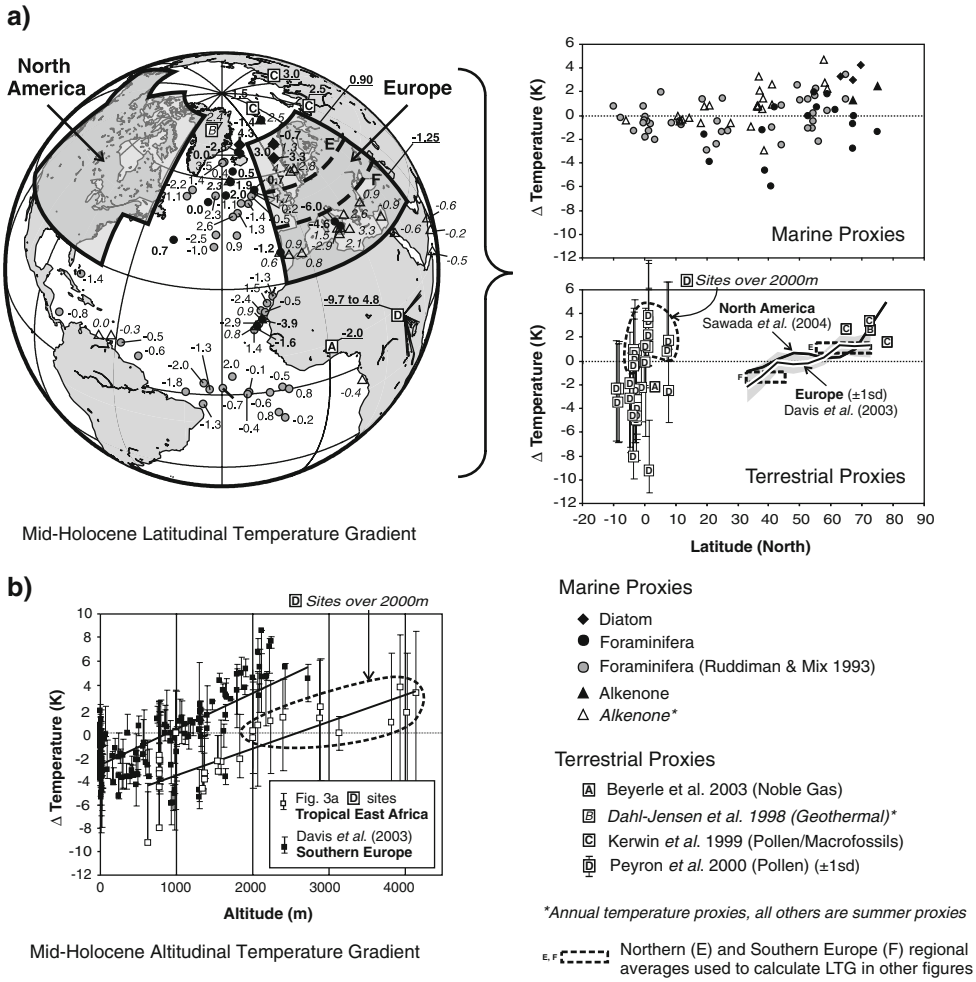

Fig. 3 Latitudinal and altitudinal temperature gradients both weakened during the mid-Holocene as a result of high latitude (altitude) warming, and low latitude (altitude) cooling. **a** Temperature anomalies are shown by latitude based on marine and terrestrial proxies reflecting summer (or in some cases annual) conditions across a major part of the Northern Hemisphere. The Ruddiman and Mix (1993) SST data is shown separately because of doubts over age-control and calibration methodology. Average latitudinal temperature anomalies are shown from north to south Europe from Davis et al. (2003), and North America from Sawada et al. (2004) (exact regions are shown on the *main map*). **b** The altitudinal gradient is based on temperature anomalies for pollen sites at different altitudes in Tropical East Africa from Peyron et al. (2000), and Southern Europe from Davis et al. (2003). Warming at low latitudes in the Tropics only occurred at sites above 2,000 m (*circled*) representing less than 13% of the total land surface, and beyond the topographic resolution of climate models

22 W/m^2, while high latitudes received more June insolation, producing a phase shift around 47°N that is also seen in the observed temperature anomalies either side of the mid-latitudes at 40–50°N.

A comparison of this observational record with the LTG simulated in climate model experiments shows how well models can reproduce this aspect of orbital forcing. Model results are shown in Fig. 4b–d for the 160°W–60°E longitude sector of the Northern Hemisphere, which is comparable with the distribution of sites in the observational record in Fig. 4a. Figure 4b shows the summer (JJA) surface temperature anomaly by latitude during the mid-Holocene for an ensemble of 16 different atmosphere-only models (A-GCM) run under the Palaeoclimate modelling intercomparison project 1 (PMIP1) framework, forced with mid-Holocene orbital configuration, pre-industrial CO_2, modern vegetation and SST's (Masson et al. 1999). Figure 4c shows the results for an ensemble of nine fully coupled Atmosphere–Ocean models (AO-GCM) run under the Palaeoclimate modelling intercomparison project 2 (PMIP2) framework, forced with mid-Holocene orbital configuration, pre-industrial CO_2 and modern vegetation (Braconnot et al. 2007a). Figure 4d shows ensemble results from three fully coupled Atmosphere–Ocean–Vegetation models (AOV-GCM), run under the same PMIP2 framework conditions, but this time the vegetation as well as the ocean has been allowed to respond interactively with the atmosphere.

Comparing Figs. 4a and b–d, it is clear that all of the climate models underestimate the extent of low latitude cooling suggested by the observations. Any low latitude cooling in the models occurs mainly between 10 and 20°N in the main Monsoon latitudes, and is notably absent in the sub-tropics and lower mid-latitudes from 20–45°N. Somewhat surprisingly, the coupled PMIP2 AO-GCM and AOV-GCM simulations show few differences with the PMIP1 models with fixed modern SST's. Differences are mainly confined to an enhanced cooling in the Monsoon regions between 10–20°N in the AO-GCM's, and notably stronger high latitude warming in all the coupled PMIP2 simulations above approximately 50°N, which better matches the observations in this region.

The contrary cooling response of low latitudes and consequent weakening of the LTG in the face of increased

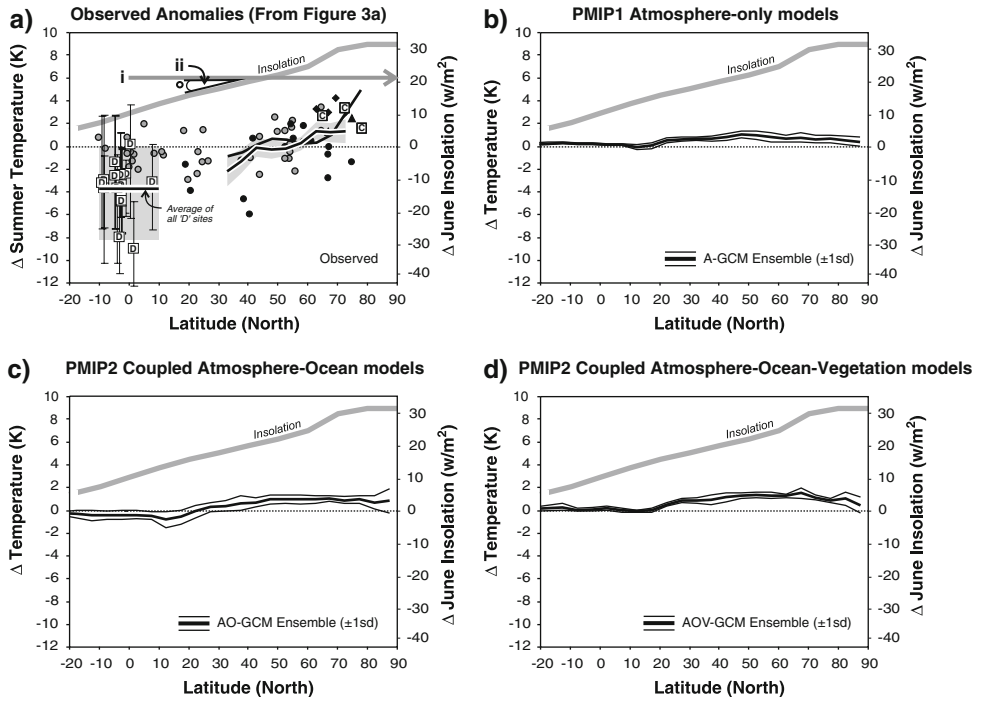

Fig. 4 A comparison of the observed and modelled mid-Holocene warmest month (summer) latitudinal temperature gradient with insolation forcing. **a** The observational data from Fig. 3a (summer temperature proxies only, and without sites over 2,000 m from Tropical East Africa as explained in the text) shows a closer agreement with the change in insolation gradient rather than direct insolation. Observed high latitude warming and low latitude cooling is not consistent with an average 22 W/m^2 increase in June insolation across all latitudes of the Northern Hemisphere (i), but is consistent with a weaker June insolation gradient, where latitudes above 47 N received higher than average insolation and those below received less than average (ii). **b**, **c** Ensemble results are shown for 16 PMIP1 Atmosphere-only (A-GCM), and 9 fully coupled Atmosphere–Ocean (AO-GCM) and 3 Atmosphere–Ocean–Vegetation (AOV-GCM) PMIP2 models, with errors calculated as 1 SD of the inter-model variance. Climate model simulations show only limited low latitude cooling in contrast to the observations, with model response indicating a warming across almost all latitudes that is more consistent with direct radiative forcing from increased insolation rather than the change in insolation gradient

summer insolation at all latitudes during the mid-Holocene appears supportive of LIG forcing, but equally, low latitude cooling can also be ascribed to other factors. The localised cooling in models associated with the tropical Monsoon zone has been explained by increased cloud cover and enhanced evaporation and convection as a consequence of a strengthened Monsoon system (Braconnot et al. 2007a). Alternatively, the decreased annual and winter insolation experienced over low latitudes at this time may have depressed sea surface temperatures so that they were unable to recover in the summer due to the thermal inertia of the ocean (Loutre et al. 2004, Rimbu et al. 2004). Evidence from the mid-Holocene and summer season alone is not therefore sufficient to demonstrate LIG forcing of the LTG, and it is for this reason that we undertook to reconstruct the LTG over the complete Holocene for both winter and summer.

2.2 Reconstructing the Holocene LTG

So far, we have compared the LTG and LIG based on a static 'snap-shot' during the mid-Holocene. A more comprehensive test of this relationship would be to compare changes in the summer/winter LTG and LIG throughout the Holocene, during which the different seasonal changes in the LIG (driven by obliquity in summer and precession in winter) could be discerned. For this long-term seasonal dynamic approach, we undertook a reconstruction of the LTG based on an existing European gridded terrestrial pollen-climate record covering the past 12,000 years compiled by Davis et al. (2003).

Traditional approaches to investigating Holocene climate have been based on single site palaeoclimate time-series or maps of palaeoclimate based on multiple sites for single time-slices, making it difficult to separate large scale orbital forcing from local scale climatic and non-climatic effects. The Davis et al. (2003) dataset however combines both time-series and mapping approaches to assimilate palaeoclimate data from multiple sites on to a uniform spatial grid at a regular time interval, allowing for the first time the energy balance of a large area of the Earths surface to be calculated and compared with orbital changes in insolation through time. This temporal–spatial approach has been applied to a pollen-based Holocene

palaeotemperature record derived from over 500 sites from across Europe (Fig. 5). Pollen data provides information on both summer and winter temperatures, allowing us to investigate seasonal temperature trends within the same dataset. Full details of the methods used in constructing the gridded record are available in Davis et al. (2003) but are summarised here.

Problems with irregular spatial and temporal sample distribution were overcome using 4-d interpolation to grid the data, a method which combines interpolation through both 3-d space and time (the 4th dimension). This data was projected on to a standardised 1° × 1° spatial grid and 100 year time-step, from which we have calculated area-average temperatures for the whole of Europe, and North and South sub-regions. Assimilation of multiple site records in this way minimises the influence of local non-climatic factors on the vegetation at each site, and maximises the background climatic signal, which underlies vegetation distribution at a continental scale. Projection on to a 3-d spatial grid that includes altitude as an independent variable also takes account of lapse rate changes, which have already been discussed. The time-step used is comparable to a smoothing running mean, and does not imply a 100-year resolution. We confine our interpretation to the millennial-scale trends, which we believe to be within the dating uncertainties inherent in the data, and anomalies are shown with respect to the most recent millenium. This gridded record has allowed us to calculate the Holocene LTG based on the difference between the reconstructed area-average temperature of the South Europe region (35–45°N) and the North Europe region (55–70°N) (areas E and F shown in Fig. 3). These two sub-regions approximately span the 47°N phase shift identified for the mid-Holocene in Fig. 4, and may be expected to be representative of low and high latitude temperature trends respectively.

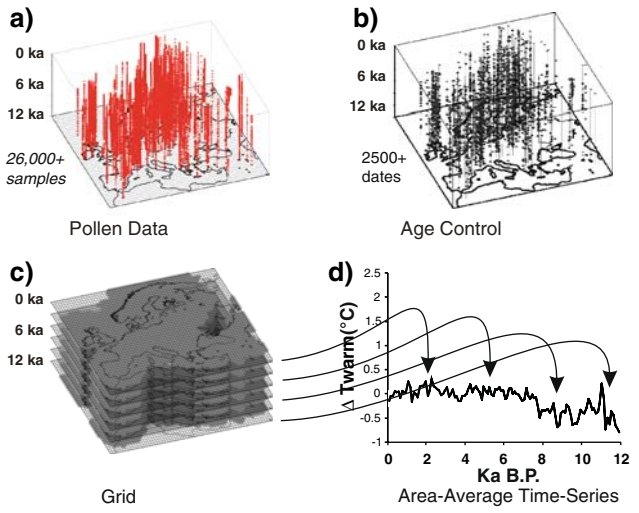

Fig. 5 Reconstruction of Holocene palaeotemperatures for the European region based on pollen data from Davis et al. (2003). **a** Paleotemperatures were calculated from over 500 pollen sites from across Europe, representing over 26,000 individual pollen samples. **b** Chronological control was provided by over 2500 calibrated absolute dates (radiocarbon, etc). **c** A modern analogue transfer function was used to convert pollen samples into temperature values, which were then interpolated on to a 3-d grid and regular time step using a 4-d technique. **d** Area-average time-series were then calculated for different spatial regions, allowing changing regional energy-balances to be viewed through time

2.3 Holocene temperature trends and the LTG/LIG

The reconstructed area average Twarm (mean temperature of the warmest month) for the entire European region (35–70°N) shows that temperatures did not respond to increased mid-Holocene summer insolation over all of Europe as might be expected (Fig. 6a). In fact, Twarm remained remarkably stable with no apparent mid-Holocene 'thermal optimum' despite a 22 W/m^2 (5%) increase in June insolation across the region at this time. In contrast, a mid-Holocene comparison of this observed record with the PMIP1 and PMIP2 model simulations at 6 ka BP shows that all models indicate summer warming at the European scale in response to increased insolation.

This overall stability of observed Holocene temperatures at the European scale represents a balance between opposing high and low latitude temperature trends (Fig. 6b). Twarm temperatures over Northern Europe show a warming consistent with the traditional idea of a mid-Holocene 'thermal optimum', while temperatures over Southern Europe show a mid-Holocene cooling. This high latitude warming and low latitude cooling is exactly the same as previously revealed in our assimilation of multiple mid-Holocene proxy records from across the Northern Hemisphere shown in Fig. 3a. Comparison with the PMIP1 and PMIP2 mid-Holocene model simulations show however that none of the models were able to reproduce this low latitude cooling observed over Southern Europe.

The LTG was calculated based on the difference in temperature between Northern and Southern Europe, as shown for summer in Fig. 6b. This shows (Fig. 7a) that high latitude warming and low latitude cooling during the mid-Holocene led to a weaker (more positive) LTG. If we overlay Holocene changes in the June LIG calculated between Northern and Southern Europe with those for the Twarm LTG, we can see that there is a good match for the latter part of the Holocene. The offset during the early part of the Holocene can be explained by residual glacial maximum ice cover, which acted to cool high latitudes and strengthen the Twarm LTG until ice cover stabilised with the disappearance of the Laurentide ice sheet around 7–8 ka BP (Peltier 1994). This explanation is made convincing by the fact that mid-late Holocene trends in December LIG

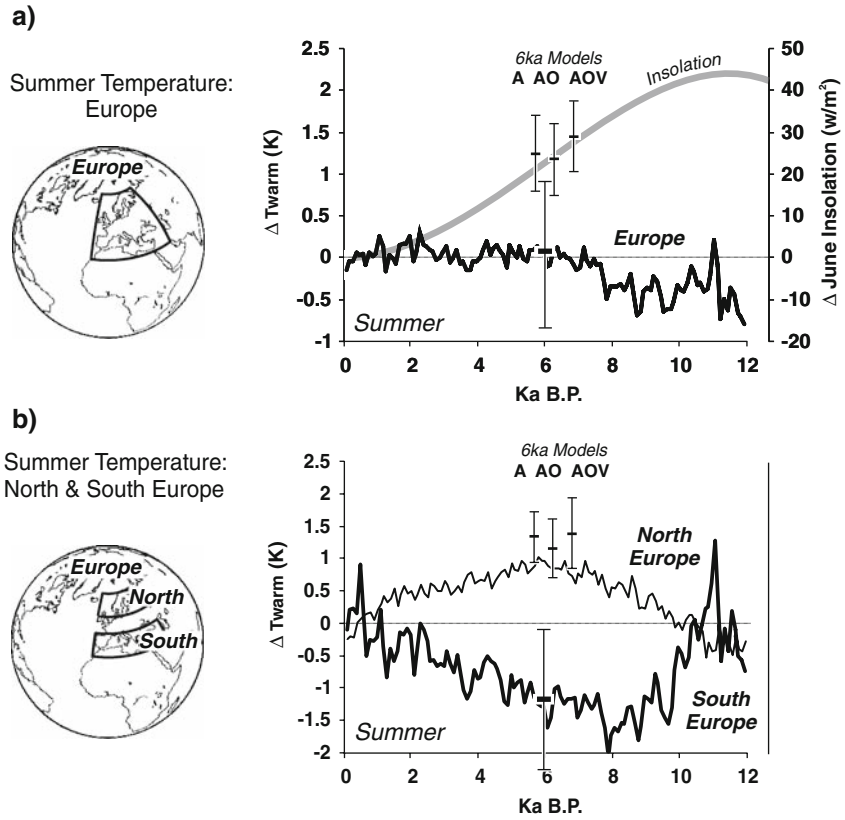

Fig. 6 Reconstructed warmest month (summer) temperatures (Twarm) for Europe during the Holocene compared with PMIP1 and PMIP2 mid-Holocene (6 ka) climate model simulations. Ensemble results are shown for 16 Atmosphere-only (*A*), and 9 fully coupled Atmosphere–Ocean (*AO*) and 3 Atmosphere–Ocean–Vegetation (*AOV*) models, with errors calculated as 1 SD of the inter-model variance. Errors are also shown for the observed temperature at 6 ka **a** The mean summer temperature of Europe shows no mid-Holocene thermal optimum in response to increased summer insolation (shown here by mean mid-month June insolation over the region from Berger 1978). In contrast, PMIP model simulations all show warming. **b** The stability of Holocene summer temperatures at the European scale represents a balance between warming over North Europe and cooling over South Europe. The low latitude cooling observed over South Europe is not reproduced in the PMIP model simulations, which all indicate low latitude warming at 6 ka

and Tcold (mean temperature of the coldest month) LTG also match (Fig. 7b), whilst at the same time being very different from those of their summer counterparts. Again, the effect of ice cover is shown to dominate the Tcold LTG during the early part of the Holocene. Figure 7a also shows the significance of the data-model mismatch highlighted in Fig. 6b, where the lack of low latitude summer cooling in the PMIP1 and PMIP2 model simulations causes models to underestimate the weakening of the summer LTG observed in the mid-Holocene. The same model simulations for the winter LTG are shown in Fig. 7b, but these are within the error bounds of the reconstruction.

2.4 The Holocene LTG and Northern Hemisphere climate

These results demonstrate systematic changes in the LTG across Europe, but do these also reflect changes in the global climate system? The LTG controls the latitudinal location of the main climate zones, including the Hadley Cell, and with it the ITCZ and Monsoon system (Flohn 1965) (Fig. 8a inset). We would therefore expect these systems to show a comparable response to the reconstructed LTG during the Holocene. The nature of this relationship is demonstrated every year as these systems migrate northwards in summer when the LTG is weak, and southward in winter when the LTG is strong. Compilations of lake level reconstructions from across North Africa indicate that water levels were highest between 10 and 6 ka, associated with a northward extension of the African Monsoon system (Jolly et al. 1998; Damnati 2000). This same period is also recorded by rapid speleothem deposition in Oman, suggesting a concurrent expansion of the Indian Monsoon (Fleitmann et al. 2003b). Figure 8a shows the timing of this mega-Monsoon together with a more continuous isotopic record of the Indian Monsoon from the Oman site (Fleitmann et al. 2003a), and a record of ITCZ position recorded in marine sediments in the southern Caribbean (Haug et al. 2001). All these observations suggest a northward expansion of the Hadley Cell during the

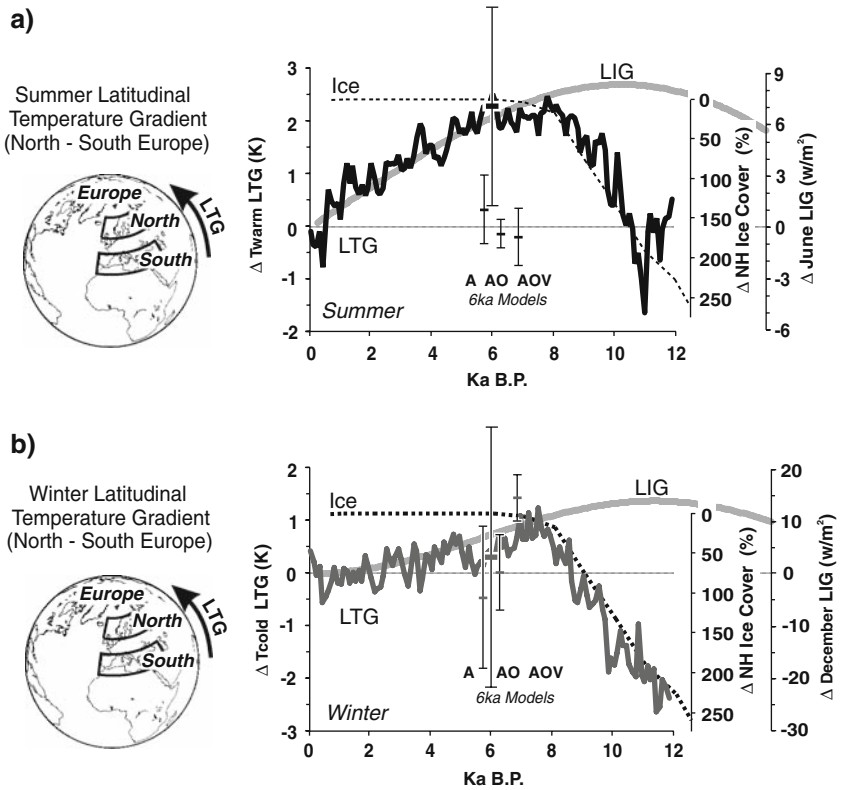

Fig. 7 Changes in seasonal reconstructed Holocene LTG can be explained by seasonal changes in LIG (mid-month values from Berger 1978), and Northern Hemisphere ice cover (from Peltier 1994). Temperature and insolation gradients were calculated by deducting mean anomaly values for Northern Europe from those of Southern Europe. **a** Summer (Twarm) LTG compared with the June LIG and ice cover. The LTG is also compared here with PMIP mid-Holocene climate model simulations, which all underestimate LTG weakening due to the lack of low latitude cooling shown in Fig. 6b. **b** Winter (Tcold) LTG compared with the December LIG and ice cover. PMIP mid-Holocene model simulations are also shown and compare more favourably with the observed LTG than in summer

Holocene consistent with our reconstruction of a weakening mid-Holocene Twarm LTG. Climate models however reproduce little change in LTG between the present day and the mid-Holocene (Fig. 7a), a factor that may explain why models continue to have difficulty reproducing the northward shift of the African Monsoon into the sub-Tropics (Joussaume et al. 1999; Braconnot et al. 2000; Valdes 2003; Braconnot et al. 2004; Braconnot et al. 2007a). One answer to this problem has been to incorporate vegetation feedbacks in AOV-GCM's, which more accurately represent these land surface changes at this time (Ganopolski et al. 1998). The change from desert to savannah lowers albedo and increases surface warming compared to AO-GCM's (as shown in Fig. 9), which helps drive convection and land–ocean temperature contrast which also boost Monsoon strength. However, the observational evidence of cooler land surface conditions may indicate that this kind of feedback is unrealistic. Similarly, evidence of cooler mid-Holocene SST's in the sub-tropical North Atlantic, although far from conclusive, would also contradict model mechanisms for enhancing the West African Monsoon based on warmer summer SST's in this region (Kutzbach and Liu 1997; Braconnot et al. 2007b). Zhao et al. (2005) have highlighted the difficulty in evaluating this mechanism, which appears to rely on a short late summer warming of SST's that may be difficult to detect in the palaeo SST record. However, irrespective of these problems, this model mechanism still fails to explain the northward extent of the African Monsoon, while appearing to cause a contradictory decrease in the strength of the Indian Monsoon (Braconnot et al. 2007b).

Evidence of extensive low latitude cooling also offers an alternative perspective for interpreting the proxy evidence of Monsoon expansion. Climate modelling experiments have focussed almost exclusively on increasing precipitation to resolve data-model discrepancies (Joussaume et al. 1999, Braconnot et al. 2007a), despite the fact that most proxies reflect positive changes in P–E that are also influenced by temperature. In this way, cooling as well as increased precipitation could equally explain the favourable shift in the moisture balance reflected in vegetation and lake-level proxies that indicate Monsoon enlargement.

Whilst the Monsoon and ITCZ are prominent summer climate modes, winter in the Northern Hemisphere is strongly influenced by the AO extra-tropical atmospheric circulation mode. The AO also includes the North Atlantic Oscillation (NAO), which we refer to herein as a regional expression of the AO. A major part of recent high latitude warming has been attributed to a shift to a more positive winter AO (Moritz et al. 2002). This change in mid-latitude westerly circulation leads to warm air advection over Northern Europe, which experiences mild wet winters, while Southern Europe experiences cool dry winters (Visbeck 2002). This higher latitude warming and lower latitude cooling leads to a weakening of the LTG across

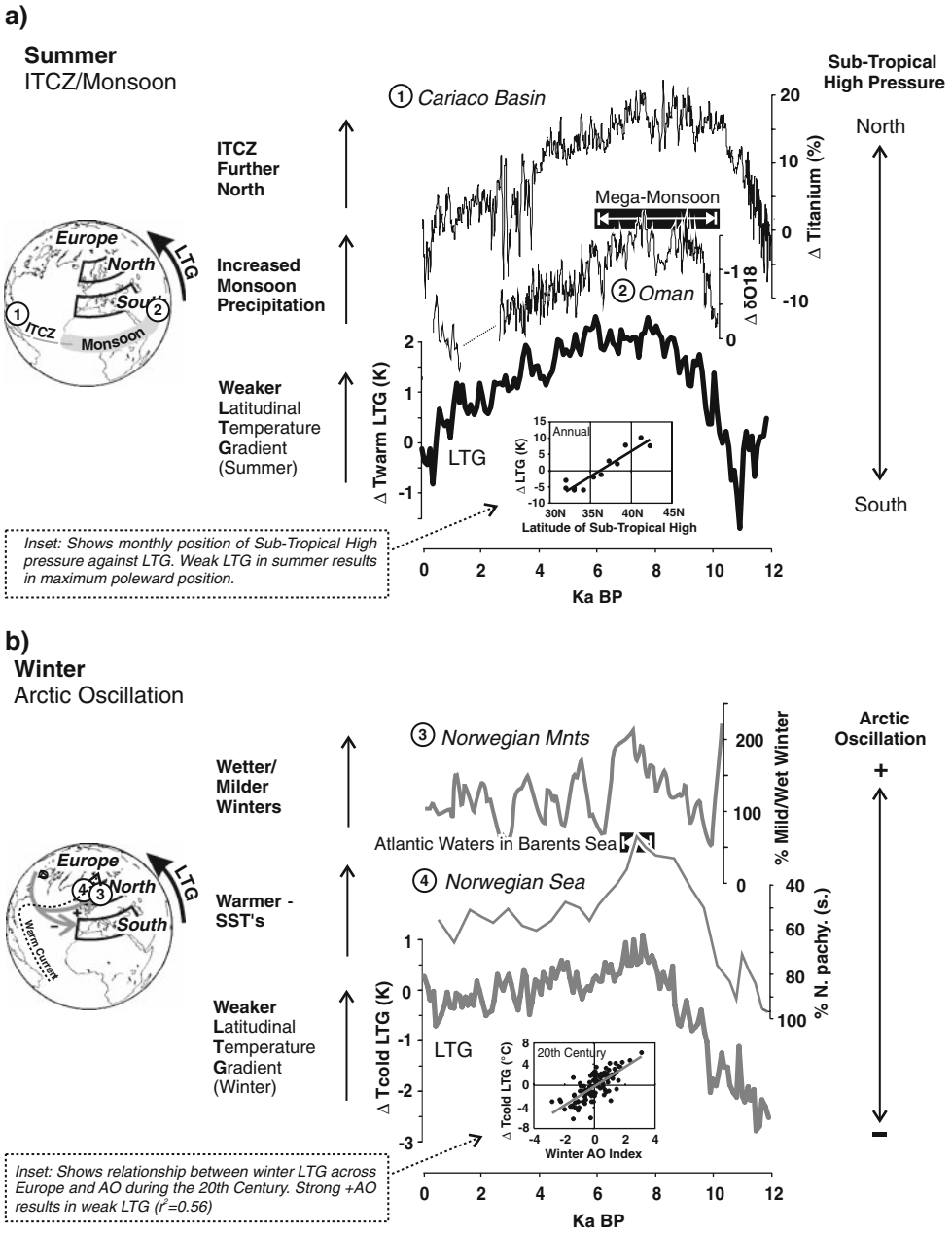

Fig. 8 A comparison of the seasonal LTG reconstructions from Fig. 7 with palaeoclimate records of the main Northern Hemisphere climate modes during the Holocene. **a** Weakening of the summer LTG during the mid-Holocene suggests a poleward displacement of the sub-tropical high pressure and Hadley Cell (Flohn 1965; see *inset*). This is supported by ① poleward displacement of the ITCZ recorded by Titanium in sediments at Cariaco Basin, Venezuela (Haug et al. 2001), as well as ② increased Monsoon intensity recorded in the isotopic composition of a speleothem at Hoti Cave, Oman (Fleitmann et al. 2003a). The black bar indicates high rates of speleothem accumulation associated with the most intense Monsoon period (Fleitmann et al. 2003b). **d** Weakening of the winter LTG during the mid-Holocene would suggest a more positive AO. Positive AO-type circulation results in warm air advection into North Europe and other high latitudes (Moritz et al. 2002), and cool air advection into South Europe (Visbeck 2002) resulting in a weakened LTG. Comparison of the twentieth century winter LTG over Europe derived from instrumental data (Mitchell et al. 2002) and the AO index (Thompson and Wallace 1999) show a strong relationship (see *inset*). The correlation value is based on the mean DJF index and the Tcold (coldest month) temperature gradient (1901–2000 AD). This is supported for the Holocene by ③ an independent reconstruction of AO (NAO) based on glacier mass-balance in Norway (Nesje et al. 2000, 2001), as well as ④ a foraminifera record from sediment core HM52-43 in the Norwegian Sea (Fronval and Jansen 1996). The decline of polar *N. pachyderma* (s.) in the mid-Holocene (note *inverted scale*) is interpreted as the result of increased northward penetration of warm Atlantic waters into the Norwegian Sea, a period that also coincides with the maximum penetration of Atlantic waters recorded in the Barents Sea (Duplessy et al. 2001) shown by the *black bar*. It has been shown the northward extent of warm Atlantic waters in this region is strongly related to wind stress arising from a positive AO (NAO) (Blindheim et al. 2000)

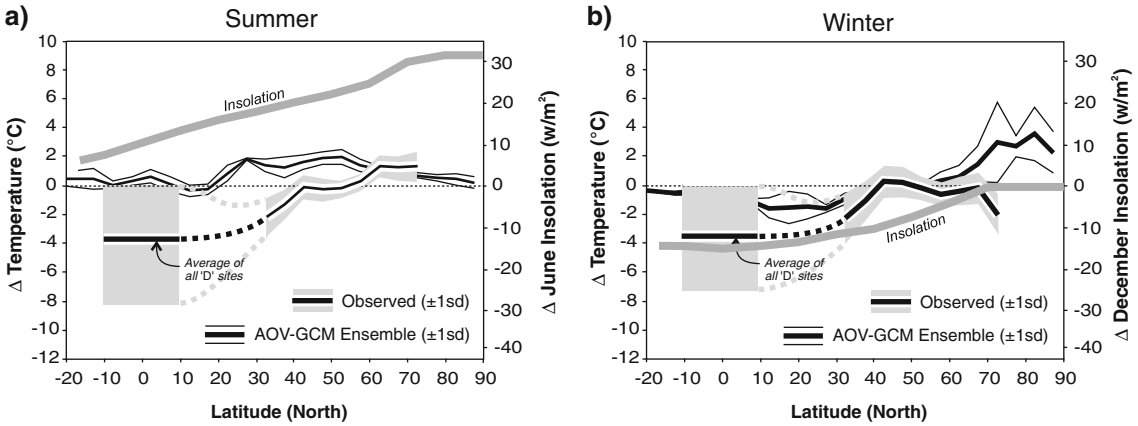

Fig. 9 A summer and winter mid-Holocene comparison of climate model and observed latitudinal temperature anomalies in the Afro-European sector (10 W–50°E), together with respective June and December insolation forcing. Analysis shows the ensemble response of 3 Atmosphere–Ocean–Vegetation (AOV) model simulations. Seasonal pollen-climate reconstructions are shown based on latitudinal average temperatures from north to south Europe, together with an average of individual sites in Tropical East Africa from Peyron et al. 2000(as shown for summer in Figs. 3 and 4a). Models over estimate low latitude warming in summer and high latitude warming in winter

Europe that is reflected in a close correlation between the Tcold LTG, and the AO during the twentieth Century ($r^2 = 0.56$) (Fig. 8b inset). We reconstruct a mid-Holocene weakening of the Tcold LTG that suggests this period was associated with a strong positive AO-type circulation. This inference is supported by the similarity between our temperature based reconstruction, and an independent reconstruction of Holocene NAO (AO) from glacier mass balance in Norway (Nesje et al. 2000; Nesje et al. 2001). Changes in the AO also influence wind stress across the North Atlantic, helping to drive warm Atlantic waters northward along the Norwegian Current during positive NAO (AO) conditions (Blindheim et al. 2000). Evidence from this region that the maximum extension of warm Atlantic waters occurred in the early mid-Holocene (Fronval and Jansen 1996; Duplessy et al. 2001) is therefore consistent with these Holocene AO (NAO) reconstructions (Fig. 8b). The change in LTG in winter is smaller than in summer, and climate model simulations are within the error-bars of the reconstruction (Fig. 7b), but model response may be expected to be closer to the observed because in winter the LIG and direct radiative forcing arise from the same insolation changes (Fig. 9). Models also appear to respond to different forcing mechanisms to that observed, with AO-GCM models showing little change in the NAO at this time (Gladstone et al. 2006). The weaker winter LTG shown in the AOV-GCM models appears to be the result of unrealistic high latitude winter warming, at least over Northern Europe (Fig. 9). This is attributed to local feedbacks such as reduced sea-ice (Ganopolski et al. 1998; Claussen 2003; Gallimore et al. 2005), and not advection processes such as the NAO.

Overall, comparison of our Holocene LTG reconstruction with a mid-Holocene multi-proxy data compilation (Fig. 3a), and records of summer Monsoon/ITCZ and winter AO climate modes (Fig. 8a, b) demonstrate that this record is representative of the Northern Hemisphere LTG. Differences in LTG trends between winter and summer also closely match trends in the LIG, consistent with LIG forcing of the LTG. Differences between the LTG and LIG in the early Holocene can be attributed to additional cooling of high latitude temperatures by residual LGM ice sheets. Following from these observations of LIG and Ice Sheet forcing of Holocene climate, further validation was undertaken through comparison of LIG and Ice Sheet forcing with climate during the earlier Eemian interglacial.

3 The Eemian interglacial

A major challenge to Milankovitch theory has come from evidence that deglaciation in the lead-up to the last interglacial (Eemian/OIS-5e) began before changes in precession had led to any significant increase in high latitude summer insolation (Gallup et al. 2002). Changes in obliquity and precession occurred together during the Holocene, but obliquity led precession into the Eemian, providing a test of our orbital forcing theory. Observed climate change during the Eemian was also very different than the Holocene, with Milankovitch theory providing little explanation as to why Eemian interglacial conditions lasted twice as long in Southern Europe as Northern Europe (Kukla 2000), or why summer and winter temperatures peaked at different times (Zagwijn 1996).

3.1 Estimating the Eemian LTG

Our initial Holocene based investigations indicated that the LTG is a function of the LIG and ice cover. We were therefore able to estimate the Eemian LTG using astronomical calculations to determine the LIG (Berger 1978), while ice cover was estimated using a marine isotope derived sea level reconstruction whose chronology was based on the U–Th dated coral record for Termination II (Waelbroeck et al. 2002). We converted sea level to Northern Hemisphere ice cover according to the Termination I deglaciation sequence (Peltier 1994) (Appendix 2). We therefore assume that the contribution to sea level by melting Northern Hemisphere ice during Termination II was the same as Termination I, as was the relationship between ice volume and surface area. Evidence indicates that higher sea levels were experienced during the Eemian than the Holocene as a result of a reduced Greenland Ice sheet. For this period, we have scaled the Eemian sea level maximum from the sea level reconstruction (+6.3 m) against a 'best estimate' of a maximum 67% reduction in the Greenland Ice sheet (Cuffey and Marshall 2000). A multiple linear regression was then used to calibrate ice cover and June/December LIG against the Twarm LTG ($r^2 = 0.82$) and Tcold LTG ($r^2 = 0.89$) respectively, based on the Holocene calibration period. The relative relationship between the different forcings and estimated/observed LTG is shown in Fig. 10. This shows that a weakening LTG (more positive) generally leads decreasing ice cover, while a strengthening LTG (more negative) leads increasing ice cover, suggesting that ice cover is being forced by the LIG through its influence on the LTG. Estimated LTG values for cold glacial periods may however be underestimated due to decreases in water vapour content and therefore the poleward flux of latent and sensible heat (Pierrehumbert 2002), although values of 9–10 K during the LGM appear comparable with estimates of 16–17 K from the Greenland deuterium ice core record located at 72 N (Masson-Delmotte et al. 2005).

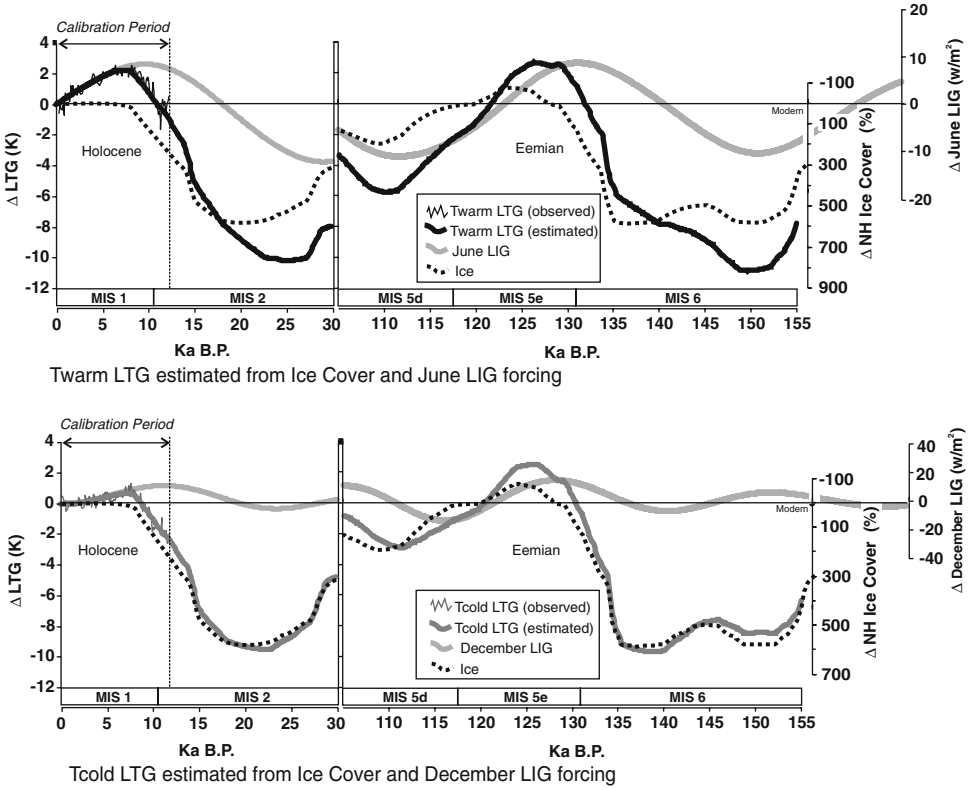

Fig. 10 Estimates of pre-Holocene summer and winter LTG were made using ice cover and LIG forcings demonstrated in Fig. 7. Calibration was undertaken over the Holocene using the observed LTG. Northern Hemisphere ice cover was calculated back to the LGM based on Peltier (1994), and thereafter estimated from the sea level reconstruction of Waelbroeck et al. (2002). Ice cover estimation is based on the relationship between sea level and Northern Hemisphere ice cover observed over the Termination I period, and therefore assumes a similar configuration of ice cover and contribution to sea level over the Termination II deglaciation period. The Termination II mid-point is taken to be 135 Ka BP, in agreement with coral evidence (Waelbroeck et al. 2002). Evidence also indicates that higher sea levels were experienced during the Eemian than the Holocene as a result of a reduced Greenland Ice sheet. For this period, we have scaled the Eemian sea level maximum from the sea level reconstruction (+6.3 m) against a 'best estimate' of a maximum 67% reduction in the Greenland Ice sheet (Cuffey and Marshall 2000). June and December LIG were derived from astronomical calculations (Berger 1978). A simple multiple linear regression was then used to calibrate ice cover and June/December LIG against Twarm LTG ($r^2 = 0.82$) and Tcold LTG ($r^2 = 0.89$) respectively, based on the Holocene calibration period

3.2 The Eemian LTG and Northern Hemisphere climate

Changes in our empirically estimated Eemian LTG (explained in Sect. 3.1) follow a different pattern from that of the Holocene, resulting in an off-set in the timing of winter and summer LTG weakening (Fig. 11b) that reflects the off-set in precession and obliquity changes (Fig. 11a). The early change in obliquity meant that the LTG weakened earlier in summer than in winter during Termination II. This would explain the earlier onset of high latitude summer warming and deglaciation indicated by the independently dated coral-based sea level evidence. Evidence of early Eemian warmth over Northern Europe is provided by the onset of rapid growth in radiometrically dated speleothems. These indicate the start of interglacial conditions at around 132 ± 5.0 ka BP in Norway (Lauritzen 1995), 133 ± 2.4 ka BP in England (Baker et al. 1995) and 135 ± 1.2 ka BP at

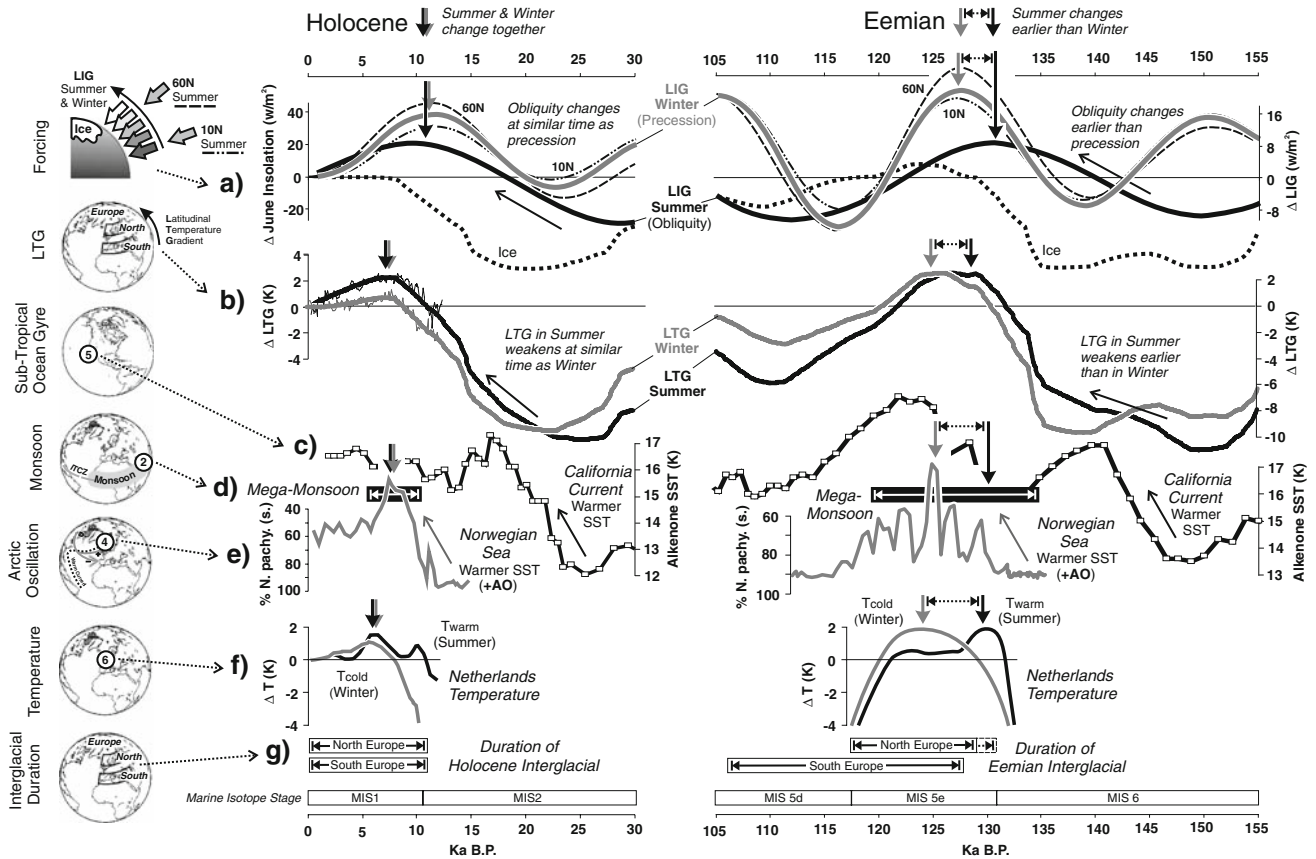

Fig. 11 LIG forcing of the LTG explains differences in winter (*grey*) and summer (*black*) climate between Holocene and Eemian interglacials (*vertical arrows*), which occurred under different orbital configurations. **a** Precession and obliquity were in phase during the Holocene, but out of phase during the Eemian (Berger 1978), resulting in similar differences in the phasing of the LIG between winter (December) and summer (June). Summer (June) insolation is shown for 60°N (*dashed line*) and 10°N (*dashed dotted line*) for comparison. Northern Hemisphere ice cover is from Fig. 9 (*dotted black line*). **b** Different phasing of precession and obliquity is reflected in the estimated LTG (from Fig. 10), which weakens earlier in summer than winter during the Eemian. **c** Early weakening of the summer LTG during the onset of the Eemian is supported by evidence of early warming of the California current (Herbert et al. 2001), which would have been influenced by the subsequent poleward shift in the sub-tropical high pressure and related ocean gyre. **d** This would also explain the early onset of 'Mega-Monsoon' conditions during the Eemian, as indicated by high rates of speleothem deposition at Hoti Cave in Oman, and dated by U–Th analysis (Fleitmann et al. 2003b). **e** The penetration of warm Atlantic waters into the Norwegian Sea recorded in two marine cores during the Holocene (HM52-43) and Eemian (ODP 644) by a decline in *N.pachy*.(s) (data and chronology from Fronval and Jansen 1996). This is interpreted as a result of a positive winter AO (see text and Fig. 8b), which was in-phase with the mega-Monsoon period during the Holocene but delayed during the Eemian. **f** Netherlands winter and summer temperatures peaked around the same time during the Holocene but summers temperatures peaked before winter temperatures during the Eemian, consistent with earlier weakening of the summer LTG. The Holocene reconstruction is pollen based (see text, Appendix 2) while the Eemian reconstruction is macrofossil based (Zagwijn 1996). Eemian chronology is based on the original authors local sea level curve adjusted to the Waelbroeck et al. (2002) reference sea level curve. **g** The duration of the Holocene and Eemian Interglacial over North and South Europe (taken from Kukla 2000) shows significant differences that indicates a strong LTG in the later Eemian, in agreement with (**b**). The chronology is taken from the author's original timescale, although the dashed extension to North Europe during the Eemian reflects the earlier warming suggested by the reference sea level curve used here and as shown in (**f**)

altitude in the Austrian Alps (Spötl et al. 2002). This evidence supports an early start to the Eemian climatic amelioration, while seasonal temperature reconstructions from the Netherlands (Zagwijn 1996) and elsewhere in Europe (Aalbersberg and Litt 1998; Rousseau et al. 2006) suggest that this warming was characterised primarily by increases in summer temperatures, while winter temperatures peaked later in the Eemian. This is different from the Holocene when summer and winter temperatures peaked at around the same time in the mid-Holocene in Northern Europe, illustrated by a pollen based temperature reconstruction for the Netherlands in Fig. 11f.

Early weakening of the summer LTG may also be reflected in low latitude records of Monsoon expansion, with U–Th dated evidence from Oman (Fleitmann et al. 2003b) indicating that Mega-Monsoon conditions became established as early as 135 Ka B.P (Fig. 11d). This predates any significant precession-driven increase in summer insolation and therefore any direct radiative forcing of the Monsoon system, but is entirely consistent with our proposed dynamic forcing of the Monsoon arising from a weakened summer LTG. The same early weakening of the summer LTG would also be expected to cause a northward shift in the sub-tropical high pressure and associated ocean gyres. This may therefore provide an explanation for early warming of the California current (Fig. 11c), which has been suggested as the main influence on the Devils Hole speleothem record (Herbert et al. 2001). The well dated record at Devils Hole has been cited as an important criticism of Milankovitch theory, since it suggests interglacial conditions began as early as 142 ± 3.0 Ka, well before any increase in high latitude summer insolation (Winograd et al. 1992; Broecker 1992; Winograd et al. 2002).

Observational evidence indicates that the latter part of Eemian MIS5e was associated with a peak in winter warming over Northern Europe associated with a wetter and more oceanic climate (Zagwijn 1996, Aalbersberg and Litt 1998). It has been suggested this oceanic climate was the result of a persistent positive AO (NAO) type circulation (Felis et al. 2004). This is in agreement with our evidence for maximum weakening of the winter LTG at this time, which also exceeds that experienced during the Holocene. The timing of this weakening and our inference that it reflects development of a strong AO-type circulation is entirely in agreement with the observed expansion of warm Atlantic waters into the Norwegian Sea at this time (Fronval and Jansen 1996) (Fig. 11e).

A significant source of debate about the Eemian has centred on the length of the interglacial itself. Estimates from Northern Europe indicate that interglacial conditions may not have extended much longer than the current Holocene, while evidence from Southern Europe indicate that warm climate conditions persisted almost twice as long again (Fig. 11 g) (Kukla 2000). This would suggest that LTG's were particularly strong in the closing stages of the Eemian (OIS-5d) as the North cooled but the South remained warm (Tzedakis 2003). Again, our model results fully support this observational evidence, indicating strong LTG's due to strong LIG's at this time (Fig. 11b). This resulted in temperature gradients across Europe that were stronger than today even when Eemian ice cover (Fig. 11a) was similar to today's levels.

4 Discussion

Glacial-interglacial cycles represent the largest changes in the Earth's climate in its recent history, yet these climatic fluctuations have occurred without any major variation in total global insolation received from the Sun. Rather, the dominant forcing has been seasonal and latitudinal variations in insolation arising from orbital changes in precession and obliquity. Understanding the climate system response to these insolation changes requires both a seasonal and latitudinal perspective, but this has generally been limited by a lack of records from low latitudes and proxies sensitive to the winter season. When viewed from both low as well as high latitudes and throughout both winter and summer seasons, the climate system response to insolation appears to be more strongly dependant on latitude than season. This suggests that summer warming of high latitudes during interglacials occurred not so much because of an increase in summer insolation, but because the increase in summer insolation was greater over high latitudes than low latitudes. This polar-amplification is not generally shown in climate models, which appear to overemphasise the seasonal rather than this latitudinal response to insolation. This suggests models underestimate the role of the LIG in driving polar amplification of global mean temperature through the LTG, and therefore may overestimate the role of Greenhouse gases in driving high latitude warming through global mean temperature over orbital timescales (Lüthi et al. 2008). The sensitivity of the LTG to LIG forcing also places greater emphasis on obliquity in summer and precession in winter in driving high latitude warming, rather than high latitude summer insolation changes, which are mainly driven by precession. This could help explain the apparent paradox of synchronous glacial–interglacial cycles between hemispheres with opposing precession-driven summer insolation receipts, because obliquity-driven summer LIG changes are in-phase between hemispheres (Fig. 12). Furthermore, many aspects of the Earth's climate are influenced by the LTG, and the sensitivity of the LTG to LIG changes could help explain the propagation of these obliquity and precession

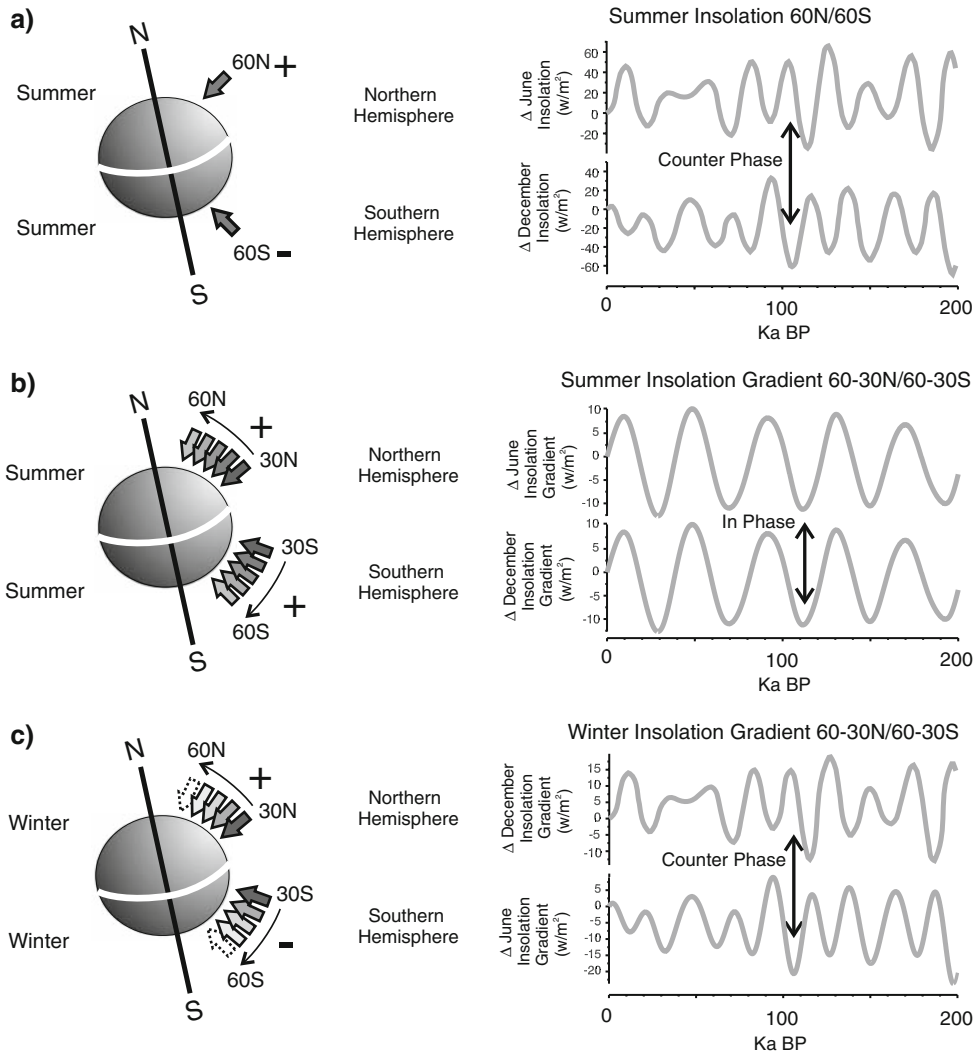

Fig. 12 The synchronisation of glacial–interglacial cycles between Northern and Southern Hemispheres suggests orbital forcing should also be in-phase. **a** High latitude summer insolation is driven by precession and is therefore in counter-phase between Hemispheres. **b** The summer insolation gradient however is driven by obliquity and is consequently in-phase in both Hemispheres. **c** The winter insolation gradient is driven by precession and is therefore out-of-phase between Hemispheres, the same as summer insolation

signatures throughout the climate system. In particular, this could explain the presence of obliquity signals in climate records at low latitudes where insolation changes are otherwise dominated by precession. In the same way, the LTG is also influenced by high latitude ice cover, which provides a way in which ice cover changes can also be overprinted on climate records from lower latitudes. The sensitivity shown by the LTG to LIG and ice cover forcing may therefore offer an alternative perspective not just on orbital forcing of high latitude warming, but also on orbital forcing of low latitude climate.

4.1 Monsoons

The Monsoon system is probably second only to the polar ice sheets in global climatic importance, and the development of mega-Monsoons are the largest climatic changes associated with non-glacial climates. As with high latitude ice sheets it is precession driven changes in summer insolation that are considered to underlie long-term orbital forcing of the Monsoon system (Rossignol-Strick et al. 1982; Kutzbach and Street-Perrott 1985). Records of Monsoon climate variability show a clear precession signal, with a contrary inter-hemispheric response that would be expected from precession forcing (Ruddiman 2006). Yet such records also include a strong obliquity signal (Clemens and Prell 2007), particularly prior to 1 million year BP when Northern Hemisphere ice sheets were poorly developed (deMenocal 1995; Lourens et al. 1996, 2001, Larrasoaña et al. 2003). This obliquity signal is difficult to explain based on simple summer insolation forcing of the Monsoon system alone. However, this response is consistent with LTG forcing of the Monsoon as a result of obliquity driven changes in the summer LIG that we identify here, particularly when the influence of ice cover on the LTG prior to 1 million year BP would have been limited. Similarly, the occurrence of major Monsoon periods at times when precessional forcing was relatively weak (Rossignol-Strick et al. 1998), but obliquity still strong, may also be explained by this mechanism.

We suggest that the intensity of summer insolation (driven by precession) influences the strength of the Monsoon system, while the LTG influences the poleward location of the Monsoon system and attendant Hadley Cell. The LTG in turn is driven by obliquity via the LIG, as well as ice cover, explaining not only the obliquity signal in Monsoon records as discussed earlier but also the non-linear response of the Monsoon to summer insolation. A weak (strong) LTG such as that associated with a decrease (increase) in high latitude ice sheets and/or weak (strong) summer LIG displaces the Monsoon system towards the pole (equator). This combination of summer insolation and LTG forcing explains the strong precession signal in Monsoon records, while also accounting for ice volume overprinting and the obliquity signal, particularly in regions on the poleward margins of the Monsoon zone. These regions would be expected to experience maximum Monsoon influence when the LTG is at its weakest, and not necessarily when summer insolation is at its strongest, accounting for some of the observed leads and lags in the insolation response where the timing of peak Monsoon intensity rarely coincides with peak summer insolation (e.g. Zabel et al. 2001; Clemens and Prell 2007). For instance, Fig. 13 shows that peak lake levels in North Africa are closely related to the early Holocene insolation maximum in the tropics, but closer to the mid-Holocene weakening of the LTG in the poleward sub-tropics. LTG control of Monsoon extent could also explain observed sub-orbital teleconnections between high latitude cooling events and aridity in Monsoon regions (Blunier et al. 1998; Gupta et al. 2003). These high latitude-cooling events would be expected to result in a (temporarily) stronger LTG, displacing the Monsoon system back towards the equator and consequently creating aridity particularly along its poleward margin.

4.2 Sub-tropical ocean gyre

The Monsoon system is related to the rising limb of the tropical Hadley Cell, while the sub-tropical high pressure and attendant sub-tropical ocean gyre is related to the falling limb of the Hadley Cell. In this way, the LTG also influences the ocean circulation as well as the Monsoon system, providing a possible basis for explaining the imprinting of obliquity periodicities and ice volume changes on low latitude SST's (deMenocal 1995; Herbert et al. 2001). A weaker LTG would displace the sub-tropical high pressure and warm sub-tropical gyre waters further poleward, whilst also reducing trade wind strength and therefore upwelling of cooler waters. For instance in a study by Wolff et al. (1999), a weakening LTG and reduced trade wind strength was forwarded to explain reduced upwelling and increasing thermocline depth in the western tropical Atlantic over the last 250 ka. This pattern was shown to vary over the 41 ka obliquity cycle, preceding ice volume changes by 3–4 ka. Similar long lead times are also found in SST records in other regions (Lea 2001), while warm gyre waters entered the California Current up to 10–15 ka ahead of ice volume changes during the late Pleistocene (Herbert et al. 2001). These examples indicate that changes in low latitude ocean circulation in some areas occurred well ahead of precession driven changes in high latitude summer insolation. Changes in the California Current in particular have been linked to the Devils Hole terrestrial speleothem record, where long and well-dated lead times have been highlighted as a criticism of Milankovitch Ice Age theory (Karner and Muller 2000). These lead times are however consistent with the proposed obliquity forcing of the sub-tropical ocean gyre via the summer LIG and LTG, as shown for the last interglacial (see Fig. 11c). In this way, the LIG would drive LTG change ahead of the ice sheets, which also

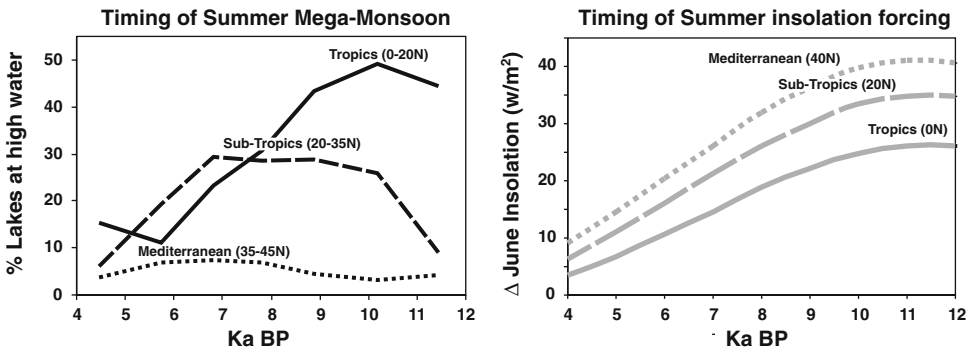

Fig. 13 The timing of peak lake levels (*left*) associated with the Holocene 'mega-Monsoon' period show a close relationship with peak insolation (*right*) close to the equator in the North African tropics. Poleward of the equator in the North African and Mediterranean sub-tropics, lakes peak after insolation, suggesting direct insolation may not be the primary forcing in these regions. Lake level data from Damnati (2000) and Harrison and Digerfeldt (1993)

modify the obliquity signal. In the absence of large ice sheets the obliquity signal would be expected to be stronger, which may explain the strong obliquity signal found in early Pleistocene California Current SST's when large Northern Hemisphere ice sheets had not yet developed (Liu and Herbert 2004).

4.3 Mid-Pleistocene change from 41 to 100 ka cycles

The development of the Northern Hemisphere ice sheets in the last 1.0–0.8 million years coincides with an important shift from an Ice Age world dominated by 41 ka cycles, to one dominated by 100 ka cycles. The origin of this shift remains unclear, but ice volume changes appear closely correlated with high latitude summer insolation over this period (Fig. 1). This includes the observation that major interglacials every 100 ka are generally coincident with peaks in high latitude summer insolation caused by modulation of the 21 ka precession signal by the 100 ka eccentricity cycle (Broecker 1992). Yet even Milankovitch acknowledged that such orbital forcing alone would be too weak to explain the observed climatic changes without operating through amplifying feedbacks. One of the main proposed feedbacks involves the ocean circulation, both directly through surface and sub-surface (thermohaline) heat transport (Imbrie et al. 1993), and indirectly through its ability to store and release CO_2 (Shackleton 2000; Ruddiman 2003). However, what is less clear are how changes in high latitude summer insolation could influence the ocean system. We have already discussed possible forcing of the sub-tropical ocean gyre through the summer LIG and LTG, the season during which the sub-tropical high pressure reaches its most poleward position. Warm salty gyre waters are then carried to higher latitudes by the mid-latitude westerly winds, which in the North Atlantic form the North Atlantic Drift and Norwegian Current that carry warm Gulf Stream waters far into Polar Regions. But maximum ocean transport by this route occurs in winter when the westerly winds are at their strongest, and particularly under positive AO (NAO) conditions when these winds have a greater southerly component that directs warm air and ocean waters northwards (Blindheim et al. 2000). The strong relationship between warm Norwegian Sea SST's, warm winters over Northern Europe, a weak winter LTG and weak winter LIG suggests LIG forcing of AO (NAO) type circulation that would promote poleward ocean transport in this region. This is essentially the same orbital forcing of the NAO as proposed by Rimbu et al. (2004), based on winter tropical insolation.

Changes in NAO (AO) associated with changes in LIG could also have wider global implications because of the strong advection of salty Atlantic waters into the Greenland and Nordic Sea areas under positive NAO (AO) conditions. This is because salty Atlantic waters in this region then cool and sink to form a major source of North Atlantic Deep Water (NADW) that drives the global thermohaline circulation. The role of NADW formation in this area was determined to be a critical factor in driving glacial–interglacial cycles by Imbrie et al. (1992, 1993). In this case, the authors saw the forcing coming from high latitude summer insolation rather than the winter LIG, but there is no contradiction in this because both forcings have almost exactly the same orbital signature (compare Figs. 1b, 2b, and Fig. 12a, c).

A further problem remains however in explaining the non-linear response to insolation that has amplified the 100 ka signal since the mid-Pleistocene. This response has been linked to the size of the continental ice sheets, which appear to modify the response to insolation forcing through a series of semi-stable states (Imbrie et al. 1993; Paillard 1998, 2001; Parrenin and Paillard 2003). Most of the major changes in ice sheet size and distribution have occurred in the North Atlantic region, which is also a key region for determining the behaviour of the thermohaline circulation. Bradley (1999, p 283) has therefore suggested that these ice sheets, and particularly the Laurentide, could have acted to significantly modify the westerly circulation as they expanded and retreated, and in turn influenced the North Atlantic ocean circulation. This mechanism could therefore add a non-linear component to the control of the mid-latitude westerly circulation and associated ocean currents that we have proposed here operating through linear changes in the winter LIG. This process may have started with the formation of a large Greenland Ice Cap around the mid-Pleistocene, when the first signs of NADW formation started to appear in the Nordic Seas, and which has been closely tied to the 100 ka cycle ever since (Henrich et al. 2002). Certainly the Greenland Ice Cap appears important in promoting local atmospheric forcing of NADW formation in the Irminger Sea associated with a positive NAO (AO) (Pickart et al. 2003), as well as maintaining storm track strength and trajectory that currently carry warmth northward to the Barents Sea (Lunt et al. 2004).

4.4 Maximum entropy production

LIG forcing of the LTG suggests a sensitivity of the climate system to small latitudinal variations in external solar forcing that does not appear to be reproduced by today's climate models. The LTG in such models is not the function of any one simple theory, but the sum of complex local and regional scale processes that determine the radiation budget at each latitude (vegetation, clouds, sea ice, etc.), as well as horizontal advective processes that move

energy between latitudes (Lindzen 1994). It therefore seems remarkable that in a system composed of such strong and independent internal processes, the LTG should be seen here to be influenced by as weak an external forcing as the LIG.

This surprising observation may therefore lend support to the controversial theory that the LTG conforms to the principle of maximum entropy production (MEP), and that despite its complexity, the LTG is in fact finely balanced to maximise entropy (Paltridge 1975; Whitfield 2005). If the principle was robust enough, and the LTG was able to remain in this steady state through time, then it could follow that the LTG would vary only in response to weak external forcing provided by the LIG, or very large internal forcing such as ice sheets. The recent application of complex GCM's to investigate MEP has highlighted the use of empirical estimates of boundary layer friction that appear to underestimate the poleward energy flux in an MEP climate (Kleidon et al. 2003). This may provide some insight into the apparent difficulty of GCM's to reproduce sufficient weakening of the mid-Holocene LTG shown here, as well as LTG's at other periods in the geological record (Pierrehumbert 2002). It remains to be seen if MEP can explain LIG forcing of the LTG, but it would appear that the apparent lack of sensitivity to this forcing shown by current climate models suggests a significant gap in our present understanding of the climate system. This may also be linked to the role of clouds and their interaction with the large scale circulation, a factor that remains one of the largest areas of uncertainty in modelling, and which could significantly affect radiative forcing of surface temperatures.

5 Conclusions

Changes in the Earth's orbital precession and obliquity influence the seasonal and latitudinal distribution of insolation, but how this orbital forcing acts on the climate system remains unclear. One of the key problems has been understanding how strong obliquity signals can underlie climatic changes commonly explained in terms of precession-driven variations in seasonal insolation, such as glacial-interglacial cycles at high latitudes and the expansion of the Monsoon system at low latitudes. A reconstruction of the Northern Hemisphere LTG during the Holocene shows that surface temperatures show an unexpectedly strong latitudinally dependant response to insolation compared to climate models, which show a stronger response to seasonal insolation. This unexpected sensitivity of the LTG to the LIG may help explain the role of obliquity, since in summer the LIG varies with obliquity. The LTG in turn influences polar amplification of global mean temperature (and hence high latitude warming), while also influencing the poleward expansion of the Hadley Cell and attendant Monsoon. In winter the LIG and LTG vary with precession, and may therefore provide an alternative explanation for precession signals in the palaeoclimate record during a season when poleward heat and moisture fluxes are at their highest. These seasonal differences in the LIG–LTG response also appear to explain differences in the timing of climatic changes between the Holocene and the Eemain interglacials, which are otherwise difficult to explain based on high latitude summer insolation alone.

Our view of orbital forcing has been largely based on a palaeoclimate record biased towards high latitudes and the summer season. By improving our knowledge of low latitudes and the winter season we may better understand the complete seasonal and latitudinal response of the climate system to insolation change, and in turn the potential importance of the LIG and LTG in driving climate change.

Acknowledgments The contribution by Simon Brewer has been funded in part by the EU MOTIF project (EVK2-2001-00263). We acknowledge the PMIP international modeling groups for providing their data for analysis and the Laboratoire des Sciences du Climat et de l'Environnement (LSCE) for collecting and archiving the model data. The PMIP2/MOTIF Data Archive is supported by CEA, CNRS, the EU project MOTIF (EVK2-CT-2002-00153) and the Programme National d'Etude de la Dynamique du Climat (PNEDC). The analyses were performed using version 11-20-2005 of the database. More information is available on http://pmip2.lsce.ipsl.fr/ and http://motif.lsce.ipsl.fr/. We also acknowledge the resources of the NOAA World Data Centre for Paleoclimatology, the PANGAEA Network for Geoscientific & Environmental Data and the European Pollen Database. We would also like to thank Odile Peyron and Carin Anderson for additional data, as well as comments on early drafts by Jed Kaplan, Erin McClymont, Takeshi Nakagawa and Tony Stevenson, as well as by two anonymous referees.

Appendices

Appendix 1

Data sources and values for mid-Holocene SST data shown in Fig. 3a, sorted first by proxy, then by latitude. The Basis coding indicates how the 6 ka temperature anomaly was calculated; (1) published linear regression equation, (2) 6 ± 0.5 ka reconstruction minus modern SST, (3) 6 ± 0.5 ka reconstruction minus 0 ± 0.5 ka reconstructed SST. The Motif SST data was kindly supplied by Carin Anderson. Pangaea data can be accessed at http://www.pangaea.de. Original data has been used where ever possible, although sources depicted by (D) have been digitised from published diagrams. Please refer to the source reference for the original references cited.

Site/Core	Lat.	Long.	Proxy	Season	Anomaly	Basis	Source	Original Reference
M23258-2/3	75.00	13.97	Alkenone	Summer	2.5	3	Marchal et al. 2002	Marchal et al. 2002 & Sarnthein et al. 2003
MD952011	66.97	7.63	Alkenone	Summer	1.3	3	Pangaea	Calvo et al. 2002
MD952015	58.76	-25.96	Alkenone	Annual	2.3	2	Pangaea	Marchal et al. 2002
IOW225514	57.84	8.70	Alkenone	Annual	2.8	1	Kim et al. 2004	Emeis et al. 2003
IOW225517	57.67	7.09	Alkenone	Annual	4.7	2	Motif	Emeis et al. 2003
AD91-17	40.87	18.64	Alkenone	Annual	2.6	1	Kim et al. 2004	Giunta et al. 2001
M44-KL71	40.84	27.76	Alkenone	Annual	0.9	1	Kim et al. 2004	Sperling et al. 2003
BS79-38	38.41	13.58	Alkenone	Annual	-2.9	2	Motif	Cacho et al. 2001
BS79-33	38.25	14.02	Alkenone	Annual	1.5	1	Marchal et al. 2002	Cacho et al. 2001
SU81-18	37.77	-10.18	Alkenone	Annual	0.6	2	Motif	Bard et al. 2000
M40-4-SL78/78MUC8	37.04	13.19	Alkenone	Annual	2.1	3	Pangaea	Emeis and Dawson 2003 & Emeis unpublished
RL11	36.75	17.72	Alkenone	Annual	3.3	2	Motif	Emeis et al. 2000
M39-008	36.38	-7.08	Alkenone	Annual	0.8	1	Kim et al. 2004	Cacho et al. 2001
GeoB 5901-2	36.38	-7.07	Alkenone	Annual	0.9	1	Kim et al. 2004	Kim et al. 2004
MD952043	36.14	-2.62	Alkenone	Annual	0.8	2	Motif	Cacho et al. 1999
ODP 967D	34.07	32.73	Alkenone	Annual	-0.9	2	Motif	Emeis et al. 2000
GeoB 5844-2	27.71	34.68	Alkenone	Annual	-0.6	1	Kim et al. 2004	Arz et al. 2003
ODP 658C	20.75	-18.58	Alkenone	Annual	0.9	2	Motif	Zhao et al. 1995 & deMenocal et al. 2000
BOFS 31K	19.00	-20.17	Alkenone	Annual	0.8	3	Chapman et al. 1996	Zhao et al. 1995 & Chapman et al. 1996
ODP 723B	18.05	57.62	Alkenone	Annual	-0.6	2	Higginson et al 2004 (D)	Higginson et al 2004
74KL	14.32	57.35	Alkenone	Annual	-0.2	1	Kim et al. 2004	Kim et al. 2004
M35003-4	12.08	-61.25	Alkenone	Annual	-0.3	3	Pangaea	Rühlemann et al. 1999
TY93-905	11.07	51.95	Alkenone	Annual	-0.5	3	Pangaea	Kim et al. 2004
ODP 1002C	10.71	-65.17	Alkenone	Annual	0.0	1	Kim et al. 2004	Herbert and Shuffert 2000 & Peterson et al. 2000
GeoB1007-4	-6.00	11.00	Alkenone	Annual	-0.4	3	Mulitza & Ruhlemann 2000 (D)	Mulitza & Ruhlemann 2000
PS21842	69.45	-16.52	Diatom	Summer	4.3	3	Pangaea	Koç et al. 1993
MD952011	66.97	7.63	Diatom	Summer	3.0	3	Marchal et. al. 2002 (D)	Koç et al. unpublished
HM79-4/6	63.10	2.55	Diatom	Summer	3.3	2	Pangaea	Koç et al. 1992
M23258-2/3	75.00	13.97	Foram	Summer	-1.4	2	Motif	Sarnthein et al. 2003
HM107-04	67.22	-19.05	Foram	Summer	0.0	2	Motif	Eirikson et al. 2000 & Knudsen et al. 2004
MD952011	66.97	7.63	Foram	Summer	-0.7	2	Motif	Andersson et al. 2003 & Risebrobakkenet al. 2003
HM107-05	66.90	-17.89	Foram	Summer	-2.8	2	Motif	Eirikson et al. 2000 & Knudsen et al. 2004
NEAP4K	61.50	-24.17	Foram	Summer	0.5	3	Marchal et. al. 2002 (D)	Marchal et. al. 2002
MD952015	58.76	-25.96	Foram	Summer	1.9	2	Motif	Marchal et al. 2002
NA87-22	55.50	-14.70	Foram	Summer	0.7	2	Motif	Duplessy 1992
NEAP17K	54.68	-28.35	Foram	Summer	2.0	2	Motif	Marchal et al. 2002
CH77-02	52.70	-36.08	Foram	Summer	0.0	2	Motif	Marchal et al. 2002
CH69-09	41.76	-47.35	Foram	Summer	0.7	1	Marchal et al. 2002	Labeyrie et al. 1999
KET80-19	40.55	13.35	Foram	Summer	-6.0	3	Kallel et al. 1997 (D)	Kallel et al. 1997
KET80-03	38.82	14.50	Foram	Summer	-4.6	3	Kallel et al. 1997 (D)	Kallel et al. 1997
SU81-18	37.77	-10.18	Foram	Summer	-1.2	1	Marchal et al. 2002	Duplessy 1992
ODP 658C	20.75	-18.58	Foram	Summer	-3.9	3	Pangaea	deMenocal et al. 2001
BOFS 31K	19.00	-20.17	Foram	Summer	-1.6	3	Chapman et al. 1996	Chapman et al. 1996
MD952011	66.97	7.63	Radiolaria	Summer	0.9	2	Pangaea	Dolven et al. 2002
V29-206	64.90	-29.28	Foram	Summer	3.50	2	Ruddiman & Mix 1993	Kellog 1984 & Ruddiman & Mix 1993
V28-14	64.78	-29.57	Foram	Summer	1.40	2	Ruddiman & Mix 1993	Kellog 1984 & Ruddiman & Mix 1993
K714-15	58.77	-25.95	Foram	Summer	0.40	2	Ruddiman & Mix 1993	Ruddiman & Mix 1996
V23-23	56.08	-44.55	Foram	Summer	-2.20	2	Ruddiman & Mix 1993	Ruddiman & Mix 1993
V27-114	55.05	-33.07	Foram	Summer	2.30	2	Ruddiman & Mix 1993	Ruddiman & Mix 1993
RC9-225	54.98	-15.40	Foram	Summer	1.70	2	Ruddiman & Mix 1993	Ruddiman et al 1977 & Ruddiman & Mix 1993
V29-192K	54.27	-16.78	Foram	Summer	0.20	2	Ruddiman & Mix 1993	Ruddiman & Mix 1993
V23-81	54.25	-16.83	Foram	Summer	-0.50	2	Ruddiman & Mix 1993	Ruddiman et al 1977
V27-20	54.00	-46.20	Foram	Summer	-1.10	2	Ruddiman & Mix 1993	Ruddiman & McIntyre 1984
V23-82	52.58	-21.93	Foram	Summer	-1.10	2	Ruddiman & Mix 1993	Sancetta et al. 1973
RC9-228	52.55	-18.75	Foram	Summer	1.40	2	Ruddiman & Mix 1993	Ruddiman et al 1977
K708-1	50.00	-23.75	Foram	Summer	1.30	2	Ruddiman & Mix 1993	Ruddiman et al 1977
V29-183K	49.13	-25.50	Foram	Summer	2.60	2	Ruddiman & Mix 1993	Ruddiman & Mix 1993
V30-101K	44.10	-32.50	Foram	Summer	-2.50	2	Ruddiman & Mix 1993	Ruddiman & Mix 1993
V29-179	44.02	-24.53	Foram	Summer	0.90	2	Ruddiman & Mix 1993	Ruddiman & McIntyre 1984 & Ruddiman & Mix 1993
V30-97	41.00	-32.93	Foram	Summer	-1.00	2	Ruddiman & Mix 1993	Ruddiman & McIntyre 1984
M12309-2	26.83	-15.12	Foram	Summer	-1.30	2	Ruddiman & Mix 1993	Thiede 1977
M12392-1	25.17	-16.85	Foram	Summer	1.50	2	Ruddiman & Mix 1993	Thiede 1977 & Mix et al. 1986
A179-15	24.80	-75.93	Foram	Summer	-1.40	2	Ruddiman & Mix 1993	Kipp 1976
M12310-4	23.50	-18.72	Foram	Summer	-0.50	2	Ruddiman & Mix 1993	Thiede 1977
M12379-1	23.13	-17.75	Foram	Summer	-2.40	2	Ruddiman & Mix 1993	Thiede 1977
V30-51K	19.87	-19.92	Foram	Summer	-2.90	2	Ruddiman & Mix 1993	Mix et al. 1986
V30-49	18.43	-21.08	Foram	Summer	1.40	2	Ruddiman & Mix 1993	Mix et al. 1986
V28-127	11.65	-80.13	Foram	Summer	-0.80	2	Ruddiman & Mix 1993	Ruddiman & Mix 1993
RC9-49	11.18	-58.58	Foram	Summer	-0.50	2	Ruddiman & Mix 1993	Be et al. 1976 & Mix et al. 1986
V25-75	8.58	-53.17	Foram	Summer	-0.60	2	Ruddiman & Mix 1993	Mix et al. 1986
V30-36	5.35	-27.32	Foram	Summer	2.00	2	Ruddiman & Mix 1993	Mix et al. 1986
V25-60	3.28	-34.83	Foram	Summer	-2.00	2	Ruddiman & Mix 1993	Mix et al. 1986
RC13-189	1.87	-30.00	Foram	Summer	-0.70	2	Ruddiman & Mix 1993	Mix et al. 1986

Appendix 2

The relationship between sea level and Northern Hemisphere ice cover during Termination I (Holocene) used to infer ice cover from sea level during Termination II (Eemian) in Figs. 10 and 11. The dashed line indicates the estimated Eemian high stand which was higher than today as a result of a reduced Greenland ice sheet.

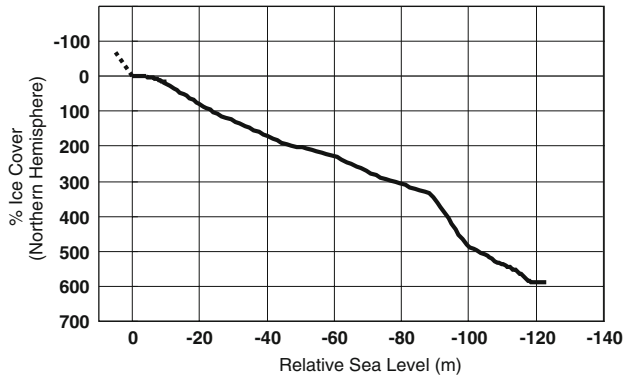

Appendix 3

Detail of Holocene pollen-climate reconstruction for Mekelermeer in the Netherlands (Bohncke et al. 1988; Bohncke and Wijmstra 1988; Bohncke 1991) shown in Fig. 11f. Analysis is based on a modern analogue technique using pollen pft scores as detailed in Davis et al. (2003). Diagram shows loess smoother in bold. Pollen data and chronology (calibrated) is from the European Pollen Database (site #547), accessed with kind permission of the author.

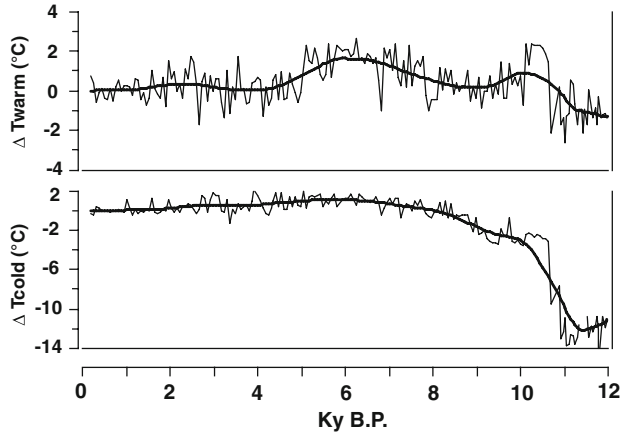

References

Aalbersberg G, Litt T (1998) Multiproxy climate reconstructions for the Eemian and Early Weichselian. J Quaternary Sci 13:367–390. doi :10.1002/(SICI)1099-1417(1998090)13:5<367::AID-JQS400>3.0.CO;2-I

Baker A, Smart PL, Edwards RL (1995) Paleoclimate implications of mass spectrometric dating of a British flowstone. Geology 23:309–312. doi :10.1130/0091-7613(1995)023<0309:PIOMSD>2.3.CO;2

Berger A (1978) Long-term variations of daily insolation and Quaternary climate changes. J Atmos Sci 35:2362–2367. doi :10.1175/1520-0469(1978)035<2362:LTVODI>2.0.CO;2

Beyerle U, Rueedi J, Leuenberger M, Aeschbach-Hertig W, Peeters F, Kipfer R, Dodo A (2003) Evidence for periods of wetter and cooler climate in the Sahel between 6 and 40 ka BP derived from groundwater. Geophys Res Lett 30(4):1173. doi:10.1029/2002GL016310

Blindheim J, Borovkov V, Hansen B, Malmberg SA, Turrell WR, Osterhus S (2000) Upper layer cooling and freshening in the Norwegian Sea in relation to atmospheric forcing. Deep Sea Res Part I Oceanogr Res Pap 47:655–680. doi:10.1016/S0967-0637(99)00070-9

Blunier T, Chappellaz J, Schwander J, Dallenbach A, Stauffer B, Stocker TF, Raynaud D, Jouzel J, Clausen HB, Hammer CU, Johnsen SJ (1998) Asynchrony of Antarctic and Greenland climate change during the last glacial period. Nature 394(6695):739–743. doi:10.1038/29447

Bohncke S (1991) Palaeohydrological changes in the Netherlands during the last 13,000 years. Thesis, Vrije University, Amsterdam, p 187

Bohncke S, Wijmstra L (1988) Reconstruction of late-glacial lake-level fluctuations in the Netherlands based on palaeobotanical analyses, geochemical results and pollen density data. Boreas 17:403–425

Bohncke S, Wijmstra L, Vanderwoude J, Sohl H (1988) The lateglacial infill of three lake successions in the Netherlands: regional vegetational history in relation to NW European vegetational developments. Boreas 17:385–402

Broecker WS (1992) Upset for Milankovitch theory. Nature 359:779–780. doi:10.1038/359779a0

Braconnot P, Joussaume S, de Noblet N, Ramstein G (2000) Mid-Holocene and Last Glacial Maximum African monsoon changes as simulated within the Palaeoclimate Modelling Intercomparison Project. Global Planet Change 26:51–66. doi:10.1016/S0921-8181(00)00033-3

Braconnot P, Harrison S, Joussaume CD, Hewitt A, Kitoh JE, Kutzbach J, Liu Z, Otto-Bliesner B, Syktus J, Weber SL (2004) Evaluation of PMIP coupled ocean–atmosphere simulations of the mid-Holocene. In: Battarbee RW, Gasse F, Stickley CE (eds) Past climate variability through Europe and Africa. Kluwer, Dordrecht, pp 515–533

Braconnot P, Otto-Bliesner B, Harrison S, Joussaume S, Peterchmitt J-Y, Abe-Ouchi A, Crucifix M, Fichefet T, Hewitt CD, Kageyamal M, Kitoh A, Loutre M-F, Marti O, Merkel U, Ramstein G, Valdes P, Weber L, Yu Y, Zhao Y (2007a) Results of PMIP2 coupled simulations of the mid-Holocene and Last Glacial Maximum—Part 1: experiments and large-scale features. Climates Past 3:261–277

Braconnot P, Otto-Bliesner B, Harrison S, Joussaume S, Peterchmitt J-Y, Abe-Ouchi A, Crucifix M, Fichefet T, Hewitt CD, Kageyamal M, Kitoh A, Loutre M-F, Marti O, Merkel U, Ramstein G, Valdes P, Weber L, Yu Y, Zhao Y (2007b) Results of PMIP2 coupled simulations of the mid-Holocene and Last Glacial Maximum—Part 2: feedbacks with emphasis on the location of the ITCZ and mid- and high latitudes heat budgets. Climates Past 3:279–296

Bradley R (1999) Paleoclimatology: reconstructing climates of the quaternary, 2nd edn. Academic Press, pp 613, ISBN 012124010X

Chapman MR, Shackleton NJ, Zhao M, Eglinton G (1996) Faunal and alkenone reconstructions of subtropical North Atlantic surface hydrology and paleotemperature over the last 28 ka. Paleoceanography 11(3):343–357. doi:10.1029/96PA00041

Claussen M (2003) Simulation of Holocene climate change using climate-system models. In: Mackay A, Battarbee R, Birks J, Oldfield F (eds) Global change in the Holocene. Arnold Publishers, ISBN 0 340 76223 3, pp 422–434

Clemens SC, Prell WL (2007) The timing of orbital-scale Indian monsoon changes. Quat Sci Rev 26:275–278. doi:10.1016/j.quascirev.2006.11.010

COHMAP members (1988) Climatic changes of the last 18,000 years. Observations and model simulations. Science 241:1043–1052

Cortijo E, Lehman S, Keigwin L, Chapman M, Paillard D, Labeyrie L (1999) Changes in meridional temperature and salinity gradients in the North Atlantic Ocean (30°–72°) during the last interglacial period. Paleoceanography 14(1):23–33

Cuffey KM, Marshall SJ (2000) Substantial contribution to sea-level rise during the last interglacial from the Greenland ice sheet. Nature 404(6778):591–594

Damnati B (2000) Holocene lake records in the Northern Hemisphere of Africa. J Afr Earth Sc 31(2):253–262

Davis BAS, Brewer S, Stevenson ACS, Guiot J, Data contributors (2003) The temperature of Europe during the Holocene reconstructed from pollen data. Quat Sci Rev 22:1701–1716

deMenocal PB (1995) Plio-Pleistocene African climate. Science 270:53–59

Duplessy J-C, Ivanova E, Murdmaa I, Paterne M, Labeyrie L (2001) Holocene paleoceanography of the northern Barents Sea and variations of the northward heat transport by the Atlantic Ocean. Boreas 30:2–16

Felis T, Lohmann G, Kuhnert H, Lorenz SJ, Scholz D, Pätzold J, Al-Rousan SA, Al-Moghrabi SM (2004) Increased seasonality in Middle East temperatures during the last interglacial period. Nature 429:164–168

Fleitmann D, Burns SJ, Mudelsee M, Neff U, Kramers J, Mangini A, Matter A (2003a) Holocene forcing of the Indian monsoon recorded in a stalagmite from Southern Oman. Science 300(5626):1737–1739

Fleitmann D, Burns SJ, Neff U, Mangini A, Matter A (2003b) Changing moisture sources over the last 330,000 years in Northern Oman from fluid-inclusion evidence in speleothems. Quatern Res 60:223–232

Flohn H (1965) Probleme der theoretischen Klimatologie. Naturwissenschaftliche Rundschau 10:385–392

Fronval T, Jansen E (1996) Rapid changes in ocean circulation and heat flux In the Nordic seas during the last interglacial period. Nature 383(6603):806–810

Gallup CD, Cheng H, Taylor FW, Edwards RL (2002) Direct determination of the timing of sea level change during Termination II. Science 295(5553):310–313

Gallimore R, Jacob R, Kutzbach J (2005) Coupled atmosphere–ocean–vegetation simulations for modern and mid-holocene climates: role of extratropical vegetation cover feedbacks. Climate Dynamics 25(7–8):755–776

Ganopolski A, Kubatzki C, Claussen M, Brovkin V, Petoukhov V (1998) The influence of vegetation–atmosphere–ocean interaction on climate during the mid-Holocene. Science 280(5371):1916–1919

Gladstone RM, Ross I, Valdes PJ, Abe-Ouchi A, Braconnot P, Brewer S, Kageyama M, Kitoh A, Legrande A, Marti O, Ohgaito R, Otto-Bliesner B, Peltier WR, Vettoretti G (2006) Mid-Holocene NAO: a PMIP2 model intercomparison. Geophys Res Lett 32(16):L16707

Gupta AK, Anderson DM, Overpeck JT (2003) Abrupt changes in the Asian southwest monsoon during the Holocene and their links to the North Atlantic Ocean. Nature 421(6921):354–357

Harrison S, Digerfeldt G (1993) European lakes as palaeohydrological and palaeoclimatic indicators. Quatern Sci Rev 12:233–248

Haug GH, Hughen KA, Sigman DM, Peterson LC, Rőhl U (2001) Southward migration of the Intertropical Convergence Zone through the Holocene. Science 293:1305–1307

Hays JD, Imbrie J, Shackleton NJ (1976) Variation in the Earth's orbit: pacemaker of the ice ages. Science 194:1121–1132

Henrich R, Baumann K-H, Huber R, Meggers H (2002) Carbonate preservation records of the past 3 Myr in the Norwegian-Greenland Sea and the northern North Atlantic: implications for the history of NADW production. Mar Geol 184:17–39

Herbert TD, Schuffert JD, Andreasen D, Heusser L, Lyle M, Mix A, Ravelo AC, Stott LD, Herguera JC (2001) Collapse of the California current during glacial maxima linked to climate change on land. Science 293(5527):71–76

Higginson MJ, Altabet MA, Wincze L, Herbert TD, Murray DW (2004) A solar (irradiance) trigger for millennial–scale abrupt changes in the southwest monsoon? Paleoceanography 19:PA3015. doi:10.1029/2004PA001,031

Howard WR (1997) A warm future in the past. Nature 388:418–419

Huntley B, Prentice IC (1988) July temperatures in Europe from pollen data, 6000 years before present. Science 241:687–690

Imbrie J, Hays JD, Martinson DG, McIntyre A, Mix AC, Morley JJ, Pisias NG, Prell WL, Shackleton NJ (1984) The orbital theory of Pleistocene climate: support from a revised chronology of the Marine del-18O record. In: Berger A, Imbrie J, Hays JD, Kukla G, Saltzman B (eds) Milankovitch and Climate, Part 1. Reidel Publishing Co., Dordrecht, pp 269–305

Imbrie J, Boyle EA, Clemens SC, Duffy A, Howard WR, Kukla G, Kutzbach JE, Martinson DG, McIntyre A, Mix AC, Molfino B, Morley JJ, Peterson LC, Pisias NG, Prell WL, Raymo ME, Shackleton NJ, Toggweiler JR (1992) On the structure and origin of major glaciation cycles, 1. Linear responses to Milankovitch forcing. Paleoceanography 7:701–738

Imbrie J, Berger A, Boyle EA, Clemens SC, Duffy A, Howard WR, Kukla G, Kutzbach J, Martinson DG, McIntyre A, Mix AC, Molfino B, Morley JJ, Peterson LC, Pisias NG, Prell WL, Raymo ME, Shackleton NJ, Toggweiler JR (1993) On the structure and origin of major glaciation cycles, 2. The 100,000-year cycle. Paleoceanography 8:699–735

Jain S, Lall U, Mann ME (1999) Seasonality and interannual variations of Northern Hemisphere temperature: equator-to-pole gradient and land-ocean contrast. J Clim 12:1086–1100

Jolly D, Harrison S, Damnati B, Bonnefille R (1998) Simulated climate and biomes of Africa during the late Quaternary: comparison with pollen and lake status data. Quatern Sci Rev 17:629–657

Joussaume S, Taylor KE, Braconnot P, Mitchell JFB, Kutzbach JE, Harrison SP, Prentice IC, Broccoli AJ, Abe-Ouchi A, Bartlein PJ, Bonfils C, Dong B, Guiot J, Herterich K, Hewitt CD, Jolly D, Kim JW, Kislov A, Kitoh A, Moutre MF, Masson V, McAvaney B, McFarlane N, de Noblet N, Peltier WR, Peterschmitt JY, Pollard D, Rind D, Royer JF, Schlesinger ME, Syktus J, Thompson S, Valdes V, Vettoretti G, Webb RS, Wyputta U (1999) Monsoon changes for 5000 years ago: results of 18 simulations from the Paleoclimate Modeling Intercomparison Project (PMIP). Geophys Res Lett 26:859–862. doi:10.1029/1999GL900126

Karner DB, Muller RA (2000) A causality problem for Milankovitch: Science 288:2143–2144

Kerwin MW, Overpeck JT, Webb RS, DeVernal A, Rind DH, Healy RJ (1999) The role of oceanic forcing in mid-Holocene Northern Hemispheric climatic change. Paleoceanography 14:200–210

Kim J-H, Rimbu N, Lorenz SJ, Lohmann G, Nam S-I, Schouten S, Rühlemann C, Schneider RR (2004) North Pacific and North Atlantic sea-surface temperature variability during the Holocene. Quat Sci Rev 23(20–22):2141–2154

Kleidon A, Fraedrich K, Kunz T, Lunkeit F (2003) The atmospheric circulation and states of maximum entropy production. Geophys Res Lett 30(23):2223

Kukla GJ (2000) The last interglacial. Science 287(5455):987–988

Kutzbach JE, Street-Perrott FA (1985) Milankovitch forcing of fluctuations in the level of tropical lakes from 18 to 0 ka BP. Nature 317:130–134

Kutzbach JE, Liu Z (1997) Response of the African monsoon to orbital forcing and ocean feedbacks in the middle Holocene. Science 278:440–443

Larrasoaña JC, Roberts AP, Rohling EJ, Winklhofer M, Wehausen R (2003) Three million years of monsoon variability over the northern Sahara. Climate Dynamics 21:689–698

Lauritzen SE (1995) High-resolution paleotemperature proxy record for the Last Interglaciation based on Norwegian speleothems. Quatern Res 43:133–146

Lea DW (2001) Ice Ages, the California Current and Devils Hole. Science 293(5527):59–60

Lindzen RS (1994) Climate dynamics and global change. Ann Revue Fluid Mech 26:353–378

Liu ZH, Herbert TD (2004) High-latitude influence on the eastern equatorial Pacific climate in the early Pleistocene epoch. Nature 427(6976):720–723

Lourens LJ, Antonarakou A, Hilgen FJ, Van Hoof AAM, Vergnaud-Grazzini C, Zachariasse WJ (1996) Evaluation of the Plio-Pleistocene astronomical timescale. Paleoceanography 11(4): 391–413

Lourens LJ, Wehausen R, Brumsack HJ (2001) Geological constraints on tidal dissipation and dynamical ellipticity of the Earth over the past three million years. Nature 409:1029–1033

Loutre M-F, Pailard D, Vimeux F, Cortijo E (2004) Does the mean annual insolation have the potential to change the climate? Earth Planet Sci Lett 221:1–14

Lunt DJ, de Noblet-Ducoudre N, Charbit S (2004) Effects of a melted greenland ice sheet on climate, vegetation, and the cryosphere. Climate Dynamics 23(7–8):679–694

Lüthi D, Le Floch M, Bereiter B, Blunier T, Barnola J-M, Siegenthaler U, Raynaud D, Jouzel J, Fischer H, Kawamura K, Stocker TF (2008) High-resolution carbon dioxide concentration record 650,000–800,000 years before present. Nature 453:379–382

Marchal O, Cacho I, Stocker T, Grimalt JO, Calvo E, Martrat B, Shackleton N, Vautravers M, Cortijo E, van Kreveld S, Andersson C, Koç N, Chapman M, Sbaffi L, Duplessy J-C, Sarnthein M, Turon J-L, Duprat J, Jansen E (2002) Apparent long-term cooling of the sea surface in the northeast Atlantic and Mediterranean during the Holocene. Quatern Sci Rev 21:455–483

Masson V, Cheddadi R, Braconnot P, Joussaume S, Texier S, PMIP-participating-groups (1999) Mid-Holocene climate in Europe: what can we infer from PMIP model-data comparisons ? Climate Dynamics 15:163–182

Masson-Delmotte V, Jouzel J, Landais A, Stievenard M, Johnsen SJ, White JWC, Werner M, Sveinbjornsdottir A, Fuhrer K (2005) GRIP Deuterium Excess reveals rapid and orbital-scale changes in Greenland Moisture Origin. Science 309(5731):118–121

Milankovitch M (1930) Mathematische Klimalehre und Astronomische Theorie der Klimaschwankungen. In: Koeppen W, Geiger R (eds) Handbuch der Klimatologie. Gebrueeder Borntraeger, Berlin, pp 1–176

Mitchell TD, Hulme M, New M (2002) Climate data for political areas. Area 34:109–112 (Dataset reference CRU TS 2.0 available at: http://www.cru.uea.ac.uk/~timm/grid/index.html)

Moritz RE, Bitz CM, Steig EJ (2002) Dynamics of recent change in the Arctic. Science 297(5586):1497–1502

Mulitza S, Ruhlemann C (2000) African Monsoonal precipitation modulated by interhemispheric temperature gradients. Quatern Res 53:270–274

Nesje A, Lie Ø, Olaf Dahl S (2000) Is the North Atlantic Oscillation reflected in Scandinavian glacier mass balance records? J Quatern Sci 15(6):587–601

Nesje A, Matthews JA, Olaf Dahl S, Berrisford MS, Andersson C (2001) Holocene glacier fluctuations of Flatebreen and winter-precipitation changes in the Jostedalsbreen region, western Norway, based on glaciolacustrine sediment records. The Holocene 11(3):267–280

Parrenin F, Paillard D (2003) Amplitude and phase of glacial cycles from a conceptual model. Earth Planet Sci Lett 214:243–250

Paillard D (1998) The timing of Pleistocene glaciations from a simple multi-state climate model. Nature 391:378–381

Paillard D (2001) Glacial cycles: toward a new paradigm. Rev Geophy 39(3):325–346

Paltridge GW (1975) Global dynamics and climate change: a system of minimum entropy exchange. Q J Royal Meteorol Soc 101: 475–484

Peixoto JP, Oort AH (1992) Physics of climate. American Institute of Physics, New York

Peltier RW (1994) Ice age paleotopography. Science 265(5169):195–201

Peyron O, Jolly D, Bonnefille R, Vincens A, Guiot J (2000) Climate of East Africa 6000 ^{14}C Yr BP as inferred from pollen data. Quatern Res 54:90–101

Pickart RS, Spall MA, Ribergaard MH, Moore GWK, Milliff RF (2003) Deep convection in the. Irminger Sea forced by the Greenland tip jet. Nature 424:152–156

Pierrehumbert RT (2002) The hydrologic cycle in deep-time problems. Nature 419(6903):191–198

Raymo ME, Nisancioglu K (2003) The 41 ka world: Milankovitch's other unsolved mystery. Paleoceanography 18(1):1011

Reijmer CH, Van Den Broeke MR, Schelle MP (2002) Air parcel trajectories and snowfall related to five deep drilling locations in Antarctica based on the ERA-15 dataset. J Clim 15:1957–1968

Rimbu N, Lohmann G, Kim J-H, Arz HW, Schneider R (2003) Arctic/North Atlantic Oscillation signature in Holocene sea surface temperature trends as obtained from alkenone data. Geophys Res Lett 30(6):1280

Rimbu N, Lohmann G, Lorenz SJ, Kim J-H, Schneider RR (2004) Holocene climate variability as derived from alkenone sea surface temperature and coupled ocean–atmosphere model experiments. Climate Dynamics 23:215–227

Rind D (1998) Latitudinal temperature gradients and climate change. J Geophys Res 103:5943–5971

Rossignol-Strick M, Nesteroff W, Olive P, Vergnaud-Grazzini C (1982) After the deluge: Mediterranean stagnation and sapropel formation. Nature 295:105–110

Rossignol-Strick M, Paterne M, Bassinot FC, Emeis K-C, de Lange GJ (1998) An unusual mid-Pleistocene monsoon period over Africa and Asia. Nature 392:269–272

Rousseau DD, Hatte Ch, Guiot J, Duzer D, Schevin P, Kukla G (2006) Reconstruction of the Grande Pile Eemian using inverse modeling of biomes and δ^{13}C. Quatern Sci Rev 25:2806–2819

Ruddiman WF (2003) Orbital insolation, ice volume, and greenhouse gases. Quatern Sci Rev 22(15):1597–1629

Ruddiman WF (2006) What is the timing of orbital-scale monsoon changes? Quatern Sci Rev 25(7–8):657–658

Ruddiman WF, Mix AC (1993) The North Atlantic and Equatorial Atlantic at 9000 and 6000 yr B.P. In: Wright HE, Kutzbach JE, Webb III T, Ruddiman WF, Street-Perrott FA, Bartlein PJ (eds) Global climates since the last glacial maximum. Holocene vegetation and climates of Europe. University of Minnesota Press, Minnesota, pp 94–124

Sawada M, Viau AE, Vettoretti G, Peltier WR, Gajewski K (2004) Comparison of North-American pollen-based temperature and global lake-status with Ccma AGCM2 output at 6 ka. Quatern Sci Rev 23:225–244

Schrag DP (2000) Climatology: of ice and elephants. Nature 404(6773):23–24
Shackleton NJ (2000) The 100,000-year ice-age cycle identified and found to lag temperature, carbon dioxide, and orbital eccentricity. Science 289:1897–1902
Spötl C, Mangini A, Frank N, Eichstädter R, Burns SJ (2002) Start of the last interglacial period at 135 ka: evidence from a high Alpine speleothem. Geology 30(9):815–818
Thompson DWJ, Wallace JM (1999) Annular modes in the extratropical circulation. Part I: month-to-month variability. J Clim 13(5):1000–1016. Data available from: http://www.atmos.colostate.edu/ao/Data/ao_index.html
Torrence C, Compo GP (1998) A practical guide to wavelet analysis. Bull Am Meteorol Soc 79:61–78
Tzedakis C (2003) Timing and duration of last interglacial conditions in Europe: a chronicle of a changing chronology. Quatern Sci Rev 22:763–768
Valdes P (2003) An introduction to climate modelling of the Holocene. In: Mackay A, Battarbee R, Birks J, Oldfield F (eds) Global change in the Holocene. Arnold Publishers, ISBN 0 340 76223 3, pp 20–35
Vimeux F, Masson V, Jouzel J, Stievenard M, Petit JR (1999) Glacial-interglacial changes in ocean surface conditions in the Southern Hemisphere. Nature 398(6726):410–413
Visbeck M (2002) The Ocean's role in Atlantic climate variability. Science 297(5590):2223–2224
Waelbroeck C, Labeyrie L, Michel E, Duplessy JC, McManus JF, Lambeck K, Balbon E, Labracherie M (2002) Sea-level and deep water temperature changes derived from benthic foraminifera isotopic records. Quatern Sci Rev 21:295–305
Whitfield J (2005) Order out of chaos. Nature 436(7053):905–907
Winograd IJ (2002) The California current, Devils hole, and Pleistocene climate. Science 296:7
Winograd IJ, Coplen TB, Landwehr JM, Riggs AC, Ludwig KR, Szabo BJ, Kolesar PT, Revesz KM (1992) Continuous 500,000-year climate record from vein calcite in Devils Hole, Nevada. Science 258:255–260
Wolff T, Mulitza S, Rühlemann C, Wefer G (1999) Response of the tropical Atlantic thermocline to late Quaternary trade wind changes. Paleoceanography 14(3):374–383
Young MA, Bradley RS (1984) Insolation gradients and the paleoclimatic record. In: Berger AL et al (eds) Milankovitch and climate Part 2. D. Reidel, Norwell, pp 707–713
Zabel M, Schneider RR, Wagner T, Adegbie AT, de Vries U, Kolonic S (2001) Late Quaternary climate changes in Central Africa as inferred from terreginous input to the Niger Fan. Quatern Res 56:207–217
Zachos J, Pagani M, Thomas E, Billups K (2001) Trends, rhythms, and aberrations in global climate 65 Ma to present. Science 292:686–693
Zagwijn WH (1996) An analysis of Eemian climate in western and central Europe. Quatern Sci Rev 15:451–469
Zhao Y, Braconnot P, Marti O, Harrison SP, Hewitt C, Kitoh A, Liu Z, Mikolajewicz U, Otto-Bliesner B, Weber SL (2005) A multi-model analysis of role of ocean feedback on the African and Indian monsoon during Mid-Holocene. Clim Dyn 25:777–800. doi:10.1007/s00382-005-0075-7